M 2014

U.PORTO
FEUP FACULDADE DE ENGENHARIA
UNIVERSIDADE DO PORTO

Complex cell-based model of intestine permeability

JOANA MARQUES E COSTA
DISSERTAÇÃO DE MESTRADO APRESENTADA
À FACULDADE DE ENGENHARIA DA UNIVERSIDADE DO PORTO EM
BIOENGENHARIA

- This page was intentionally left blank. -

U.PORTO

INSTITUTO DE CIÊNCIAS BIOMÉDICAS ABEL SALAZAR
UNIVERSIDADE DO PORTO

Faculdade de Engenharia da Universidade do Porto

Instituto de Ciências Biomédicas Abel Salazar

Complex cell-based model of intestine permeability

Joana Marques e Costa

Master Thesis
Submitted in partial fulfilment
of the requirements for the Degree of
Master of Science in Bioengineering,
at the Faculdade de Engenharia da Universidade do Porto
and Instituto de Ciências Biomédicas Abel Salazar
Advisor: Prof. Dr. Pedro Ganja
Co-advisor: Prof. Dr. Bruno Sarmento

September 2014

Abstract

In vitro cell models are widely used tools to screen the absorption and pharmacokinetics of new drugs. In the case of oral administration, the intestinal *in vitro* cell models are usually based on Caco-2 cells, which may differentiate into enterocytes-like cells after 21-days on culture.

One of the referred improved *in vitro* intestinal models consists in a co-culture system of Caco-2 cells and Raji B lymphocytes. The rationale behind it is supported by the observations of a phenotypic shift on Caco-2 cells into M cell-like cells induced by the lymphocytes. M cells are a specific epithelial cell type specialized in transepithelial transport of macromolecules, particles, and microorganisms, generally present in mucosa-associated lymphoid tissues.

With the aim of studying such transdifferentiation mechanism using a less time consuming cell model, this project consists in the assessment of a 7-days co-culture model of Caco-2 and Raji B cells. In order to do so, several experiments were performed in four models, namely 7-days Caco-2 monoculture, 7-days Caco-2:Raji B co-culture, 21-days Caco-2 monoculture and 21-days Caco-2:Raji B co-culture. The goal was to assess characteristics of the models and validate the 7-days models by comparison with the settled 21-days one.

The first parameter to be assessed was cell monolayer integrity by the transepithelial electrical resistance (TEER) and the performance of paracellular permeability studies. These revealed that although the TEER values of the 7-days model are lower, all of the four model showed their cell monolayer intact. Then, a permeability study was performed with insulin as model drug aiming to assess the permeation capability of the models. The obtained values were satisfactory when comparing to others in the literature and there was no permeation difference between any of the models. Regarding cell morphology and phenotype, traits of differentiated cells were analyzed by microscopic techniques, as the presence of tight junctions and microvilli

and also the expression of occludin, a tight junction protein, and alkaline phosphatase, a digestive enzyme. It was also examined the presence of galectin-9, a lectin that was reported as a specific marker for M cells. These experiments revealed that all the differentiated cell features analyzed were found in the 7-days models as in the 21-days models, with exception of galectin-9 whose labeling is still being optimized. Additionally the enzymatic activity of alkaline phosphatase, that is a more reliable indicator of cell differentiation, was also assessed. With this assay, differences were found between the 7-days models and the 21-days models, which exhibited higher activity. In all the studies performed, no significant variations between the mono and co-cultures were detected, pointing out that the phenotypic shift may have been too subtle to be perceived. As an outcome of this project there is the evaluation of the 7-days Caco-2 mono-culture that seems to be a model capable of resembling the intestinal epithelium as a dynamic barrier. Regarding the co-culture model, more studies are necessary to optimize de procedures and then validate the M cell-like transdifferentiation ability of the model.

Acknowledgments

First of all, I would like to thank to my advisor, Dr. Pedro Granja, for giving me the amazing opportunity of making part of INEB, kindly welcoming me in his team, always sharing positivism. I also express my deepest gratitude to my thesis co-advisor, Dr. Bruno Sarmento, for the provided guidance and support, and also for motivating me to look optimistically to my research whether things go as planned or not – that was a precious lesson.

Secondly, I am grateful to my team headed by Bruno Sarmento and also to BioCarrier group for creating such a great working environment. Here, I express my gratitude individually to: Sílvia Bidarra, for lending me a lot of material that was crucial to get my results in time; Pedro Fonte, for kindly perform the quantification of insulin samples; and the last, but not the least, to Carla Pereira, who was a mentor in the beginning of my work, helping me tirelessly whenever I needed.

To all INEB people, for welcoming me in the family and for inspiring me every day. Among these people I have a special acknowledgment to my friends of the -1.17 room with whom I shared the ups and downs of this experience. Without them this journey would not have been as exceptional.

Foremost, I would like to mention my family and my closest friends, especially my parents, for always supporting me and for making possible everything I ever did. For them, there is no possible fair acknowledgment, because no such thing can be put in words.

- This page was intentionally left blank. -

Table of Contents

List of Figures

- This page was intentionally left blank. -

List of Tables

- This page was intentionally left blank. -

Glossary

ALP – Akaline phosphatase

BALT – Bronchus-associated lymphoid tissue

DMEM – Dulbecco's modified eagle's medium

ETS - E26 transformation-specific

FAE – Follicle-associated epithelium

FBS – Fetal bovine serum

FITC – Fluorescein isothiocyanate

GALT – Gut-associated lymphoid tissue

GI – Gastrointestinal

GP2 – Glycoprotein 2

HMDS - Hexamethyldisilazane

Lgr5 – Leucine-rich repeat-containing G protein-coupled receptor

LT – Lymphotoxin

M – Microfold

MALT – Mucosa-associated lymphoid tissue

MIF – Migration inhibitory factor

NALT – Nasopharyngeal-associated lymphoid tissue

NF-kB – Nuclear factor Kappa-light-chain-enhancer of activated B cells

PBS – Phosphate buffered saline

PFA – Paraformaldehyde

PP – Peyer's patches

RANK – Receptor Activator of NF-kB

RANKL – Receptor Activator of NF-kB ligand

SEM – Scanning Electron Microscopy

TEER – Transepithelial electrical resistance

TEM – Transmission Electron Microscopy

TJ – Tight junction

TNF – Tumor Necrosis Factor

UEA-1 – Ulex europaeusagglutinin 1

Chapter 1

Outline

This document is divided into four chapters. Firstly, a general view of the scientific background supporting this project is presented in C**hapter 2 – Introduction,** as well as the objectives of the work**. Chapter 3** describes the aim of the present thesis**.** In **Chapter 4 – Materials and Methods** - all the methodology used to perform the experiments can be found. In **Chapter 5 – Results and Discussion –** all the relevant results are described and analysed. The implications of the data obtained during the project are also scrutinized in these chapter. Finally, the main results are highlighted and suggestions for future work are presented in **Chapter 6 – Conclusions.**

- This page was intentionally left blank. -

Chapter 2

Introduction

2.1. The Intestine

The intestine is responsible for the digestion and absorption of nutrients and it has also the functions of secreting molecules and carrying out immunoresponses. These process are facilitated by the unique structure of the intestine that comprises several levels of infolding resulting in a vast surface area, which allows maximal nutrient absorption[1]. In fact, 90% of the absorption sites in the gastrointestinal (GI) tract occur in the small intestine and the presence of villi and microvilli increase the surface area by 30-fold to 600-fold, respectively[2].

The wall of the intestine is divided, as any other segment of the GI tract, into four layers that are connected by connective tissue and neural and vascular components: the mucosa, the submucosa, the muscularis propria, and the serosa[1].

The innermost and also the most complex layer is the mucosa, where the absorptive function takes place. By its turn, it comprises three layers: the first layer in contact with the intestinal lumen is the epithelium, which is a single layer of epithelial cells; the second layer is the lamina propria, that contains subepithelial connective tissue, blood capillaries and lymph nodes; the third and deepest layer is the muscularis mucosae, a thin layer of smooth muscle[1,3].

The intestinal epithelium is the most self-renewing tissue of adult mammals[4]. It is composed by enteroendocrine cells, Paneth cells, goblet cells, enterocytes (that make up more than 80% of all intestinal cells) and microfold (M) cells which will be extensively reviewed further ahead. The enteroendocrine cells coordinate gut functioning through specific hormonal secretion; Paneth cells reside at the crypts and have a role in innate immunity by secreting proteins such as antimicrobials and defensins; goblet cells produce and secrete mucins, which constitute the

mucus required for the chemical and mechanical protection of the gut; enterocytes represent the absorptive lineage and are columnar cells, highly polarized, with an apical brush border that absorbs nutrients across the epithelium[3].

Since the intestinal epithelium itself represents the biggest barrier to the ingested foreign substances[2] and participates in the innate immunity, it is associated to a lymphoid tissue. In fact, the intestinal mucosa contain organized immune inductive tissues, collectively referred as mucosa-associated lymphoid tissue (MALT), which can disseminate T and B cells after antigenic stimulation. MALT typically consists of lymphoid follicles having distinct T and B-cell areas with germinal centers, as well as dendritic cells, overlaid by a specialized follicle-associated epithelium (FAE)[5]. Depending on the localization in the organism there are different version of MALT. In the intestine one should refer to the gut-associated lymphoid tissue (GALT). More specifically, Peyer's patches (PP) are lymphoid follicles on the wall of the intestine projecting themselves into the lumen forming dome shapes[6,7]. The distinct feature of FAE overlying the PP's dome is that it contains M cells. These cells are specialized in the uptake and sampling of antigens, being approximately 10% of PP's FAE in humans[6,8].

2.1.1. Mechanisms of intestinal uptake

There are several routes of uptake regarding the intestinal epithelium. Small and amphiphatic molecules can cross the epithelial cell layer by passive diffusion since they can partion into the lipid bilayers. By its turn, low molecular weight hydrophilic molecules can cross the epithelial cell layer by the paracellular route, or by uptake of fluids. Also, there several specialized transporters to perform facilitated uptake of molecules such as sugar, aminoacids, among others[9]. Regarding larger molecules as peptides and proteins (some of interest to the drug delivery), these can be absorbed by endocytic events[10].

Concerning the endocytic uptake, it has been described four elucidated mechanisms in epithelial cells: clathrin-mediated endocytosis, phagocytosis, micropinocytosis and caveolin-mediated endocytosis. The first ones are both mechanisms mediated by receptors[11]. Macropinocytosis is an active process, depending on actin, in which large volumes of fluid may be internalized[12]. The invaginations named caveolae have only be found in the basolateral membrane of epithelial cells[13].

In respect to the absorptive cells, enterocytes commonly take up proteins by clathrin-mediated endocytosis[10], but it has been described that they may also be capable of taking up particles through phagocytosis[14]. On the other hand, it has been described that M cells are capable of performing transepithelial transport of substances by fluid-phase or receptor-mediated endocytosis at the apical membrane[8]. Then, the particles are transported in vesicles

across the cytoplasm and suffer exocytosis on the basolateral membrane[7,8,15]. This whole process of uptake, transport across the cell and exocytosis is called transcytosis.

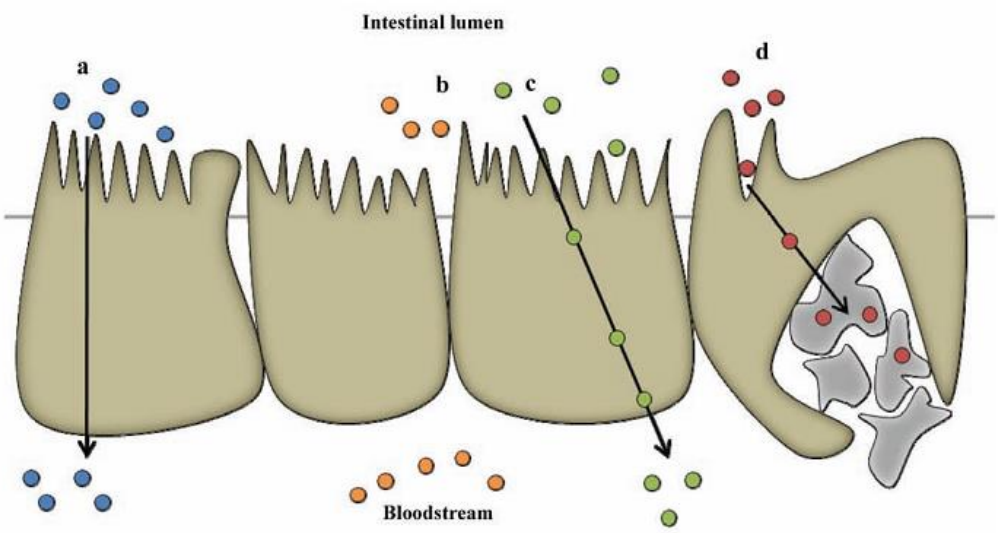

Figure 1 - Schematic illustration of Schematic representation of the intestinal epithelium and the pathways fir drug absorption. a) Transcellular pathway. b) Paracellular pathway. c) Transcytosis and receptor-mediated endocytosis. d) Absorption into the lymphatic circulation via M-cells of Peyer's patches. Adapted from *Antunes et al*, 2013[16]

It is of special interest to note that the FAE is considered a break in the intestinal barrier to macromolecules by presenting lower enzyme activity, less mucus and increased endocytic capacity[17].

2.2. M cells

M cells combine two important functions: maintenance of the barrier and the transport and sampling of luminal antigens, triggering the immune response at the mucosa level.

2.2.1. Characteristics of M cells

M cells present site- and species-related variation but they are generally characterized by specific features, namely the sparse and irregular microvilli on their apical surface, the basolateral pocket containing lymphocytes or macrophages, absence of a thick glycocalix layer and the ability to transport a wide range of materials associated with a high transcytotic capacity [6-8,15,18]. These unique features make M cells able to perform luminal antigen sampling so that cells of the immune system contact with potential pathogens. Lymphatic dissemination is the broadly documented faith of the particles taken by M cells in PP. The particles are

transported to the mesenteric lymph nodes and might be able to disseminate via the lymphatic vessels to the systemic circulation[8,19,20]. All together these characteristics make M cells attractive targets for oral drug and nanoparticle delivery studies[8,18].

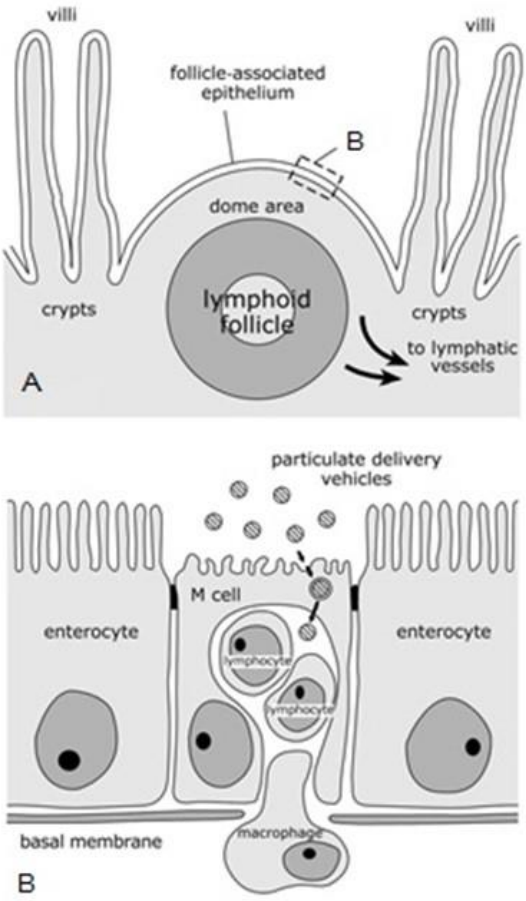

Figure 2 – Schematic representation of sections of a Peyer's patch lymphoid follicle and overlying follicle-associated epithelium (FAE).The structure of intestinal organized mucosa-associated lymphoid tissues is represented by the transverse section of a Peyer's patch lymphoid follicle (A). The lymphoid follicle is situated beneath a dome area which goes into the gut lumen between villi and which is covered by the FAE. This epithelium is characterized by the presence of M cells which possess a reduced number of irregular microvilli on their apical surface and a basolateral cytoplasmic invagination which creates a pocket for lymphocytes and macrophages. Adapted from *Clark et al*, 2001[8].

Additionally, some of the pathogenic microorganisms, such as *Salmonella*[21], *Yersinia*[22], *Mycobacterium*[23], and reovirus[24] have evolved mechanisms to exploit M cells as a portal to infect the host's organism.

M cell targeting has been provided in animal models, using targeting molecules such as the fucose binding lectin Ulex europaeusagglutinin 1 (UEA-1), and the sigma protein from reovirus. However these molecules are only specific to mouse M cells[25]. Indeed, many efforts have been made to discover cellular markers of human M cells. Human M cell markers would allow specific delivery of antigens in order to improve the efficacy of mucosal vaccines or drug carriers (M cells in drug and vaccine delivery is extensively reviewed elsewhere[8]). In that sense, studies

using microarray analyses and an M cell-like model have shown that galectin-9[26], sialyl-Lewis A antigen[27], and clusterin[28] are specific for human intestinal M cells.

2.2.2. Hypothesis on M cell genesis

In the intestine, almost all epithelial cell lineages develop from intestinal epithelial stem cells within the crypts: the dome-associated crypts surrounding the FAE and the villous crypts at the base of the villi. Thereby studies have confirmed that FAE cells, including M cells, are derived from the $Lgr5^+$ (leucine-rich repeat-containing G protein-coupled receptor) stem cells within the dome-associated crypts [29-32]. Studies suggest that LGR5 may be a marker for stem cells in small and large intestines. Moreover, using genetic approaches, it was demonstrated that LGR5-positive crypt base columnar cells are multipotent for all mature intestinal epithelial cell types[33,34].

However, it is still controversial whether M cells arise as a separate cell line or differentiate from enterocytes under the influence of immune cells that lie in the dome epithelium[15,32,35].

The first hypothesis defends that M cell formation is restricted to specialized dome associated crypts, where a subpopulation is pre-determined as M cells before attaining their morphological and functional features, as it was suggested in the works of *Gebert et al*[32] and *Lelouard et al*[36]. The hypothesis that M cells differentiate from enterocytes was firstly proposed by *Smith et al*[37] and *Bhalla et al*[38].

In both theories, there are studies supporting that the commitment to the intestinal M-cell linage is dependent on the action of the cytokine Receptor Activator of NF-kB Ligand (RANKL). RANKL is selectively expressed by stromal cells in the sub-epithelial dome region beneath the FAE of PP [39]. RANKL together with its receptor activator of NF-kB (RANK), expressed by FAE cells, are a cognate pair of the Tumor Necrosis Factor (TNF) receptor/ligand superfamilies[40]. RANKL not only induces M cell specific markers such as the glycoprotein 2 (GP2), but it also strongly regulates Spi-B[30,41], a transcription factor from the E26 transformation-specific (ETS) family[42].

Although immature M-cell differentiation appeared to be unaffected in Spi-B-deficient (Spi-$B^{-/-}$) mice, their FAE were almost completely deficient in functionally mature M cells[10,16] indicating that the differentiation of these cells, as for other intestinal epithelial cell lineages, is regulated by a specific transcription factor[41]. *Sato et al* have also investigated the requirement for Spi-B in M-cell through the detection of specific M cells markers. Though the expression of the mature GP2+ M cells was completely absent in the FAE of Spi-B-/- mice, a small number of sites of α-1,2 fucosylation (another M cell-like feature) was evident. This

suggests that a small population of M cells in the FAE may mature independently of Spi-B and as consequence do not express proteins such as GP2 on their surfaces[43].

On the other hand, some works have reported an increase in the number of M cells and enhanced transcytosis activity within the FAE after microbial challenge. One of the first reported showed that *Salmonella Typhimurium* caused an increase in the number of M cells in mouse FAE within 12 hours of infection, that would be differentiated enterocytes[44]. The possible role of pathogens in the formation of M cells will be explored further ahead.

The theory that M cells differentiate from enterocytes was also supported by findings of *Kernéis et al*[45] and later also by *Araújo et al*[35], where interaction of the epithelial cell line Caco-2 with lymphocytes led to the formation of M-cell-like cells that resembled intestinal M cells functions and morphology. However, insights on the chemomediators involved in this phenotype acquisition are not identified. In addition, some in vivo studies have brought up evidences that M cell genesis is indeed immunoregulated: bone marrow transplantation in severe combined immunodeficient mice induced the formation of M cells[46]; B cells participated in the formation of both FAE and M cells in knockout mice experiments[47].

2.2.2.1. The role of immune cells

The theory of lymphocyte induced M cell formation raises the question of how exactly can lymphoid cells transform an enterocyte into an M cell. The molecular events are still unclear but the referred data seems to demonstrate that M cells development is controlled by lymphoepithelial cross talk. In fact, in the small intestine, the chemokine CCL20 is specifically expressed by the FAE and in the PP it mediates the chemoattraction of CCR6 (C-C motif chemokine receptor 6) expressing lymphocytes and leukocytes[48,49]. In a study by *Ebisawa et al* it was reported that a specific subset of $CCR6^{hi}CD11c^{int}$ B cells migrates towards CCL20 produced by FAE and promotes M-cell differentiation. In mice lacking CCR6, the referred subset of B cells could not migrate towards the FAE and M-cell differentiation was impaired[50]. An interesting fact about CCL20 is that the previously cited study also reported that the CCL20–CCR6 and RANKL–RANK systems are regulated independently of each other[50], whereas *Mabbott et al* reports that the expression of CCL20 in the intestinal epithelium is rapidly induced by RANKL stimulation[31]. So, RANKL may not only stimulate M cells differentiation through direct contact with M cells precursors (in a Spi-B dependent manner) but also/or through CCL20-mediated attraction of B cells to the FAE region. Nevertheless, further analysis points out that while mature M cells are dramatically reduced in the FAE of CCR6-/- mice, immature M cells are maintained, implying that CCL20-CCR6 signaling does not influence the initial M-cell differentiation but instead hampers their functional maturation[50,51].

Moreover, some other cytokines of the TNF family – lymphotoxin (LT)α, LTβ and TNF – which play an important role in the formation of peripherial lymphoid tissues[52], have been investigated in the scope of M cell organogenesis. More specifically, it was reported that stimulation of TNF and LTβ receptors enhanced the expression of CCL20 in intestinal epithelial cells[53,54]. Additionally, another study from *Hsieh et al* showed that the treatment with TNFα and LTβ receptor agonist strongly induced the transcription of the TNF receptor superfamily member CD137 by epithelial intestinal cells[55]. Some authors claim that CD137/CD137L signaling between M cell progenitors and basolateral pocket B cells may provide at least one of the signals that induce final functional maturation of developing M cells[55,56]. Such event may explain how B cells could interact with M cell precursors, but it is still a subject not fully clarified.

Regarding the role of the cytokines TNF and LTβ, once they may stimulate the expression of CCL20 and CD137 molecules, one could propose that they may trigger M cell development. One interesting aspect of the mentioned lymphotoxins is that they may be also supplied by non-lymphocyte cells, as it was proposed by *Debard et al*, since lymphocytes were required for the complete formation of FAE but their absence did not prevent the development of M cells[57].

2.2.2.2.The role of pathogens

Cells exhibiting features of M cells that were not in contact with lymphocytes were observed in other experiments. It is the case of some enteroinvasive bacteria, including *Salmonella Typhimurium* and the pathogenic bacteria *Salmonella Enteritidis* and *Listeria monocytogenes* that have been shown to induce CCL20 expression by intestinal epithelial cells[58]. This could be either a host response to infection in an attempt to enhance the immunosurveillance of the gut lumen, or a way for these pathogens to infect the host by stimulating the differentiation of enterocytes into M cells, guaranteeing their uptake[31]. Similarly, other pathogens have been stated to induce rapid (less than one hour) formation of vimentin-positive M cells in rabbit PPs[59]. Vimentin is a well-established sensitive marker for M-cells in rabbit MALT[60,61]. More recently, *Tahoun et al* used *in vivo* and *in vitro* models of infection with *Salmonella* and M cell number increased as soon as 90 minutes[62]. These data

together suggest that due to the sudden increase of M cells, synthesis of these cells from lineage-specific stem cells in follicle associated crypts is highly unlikely[62].

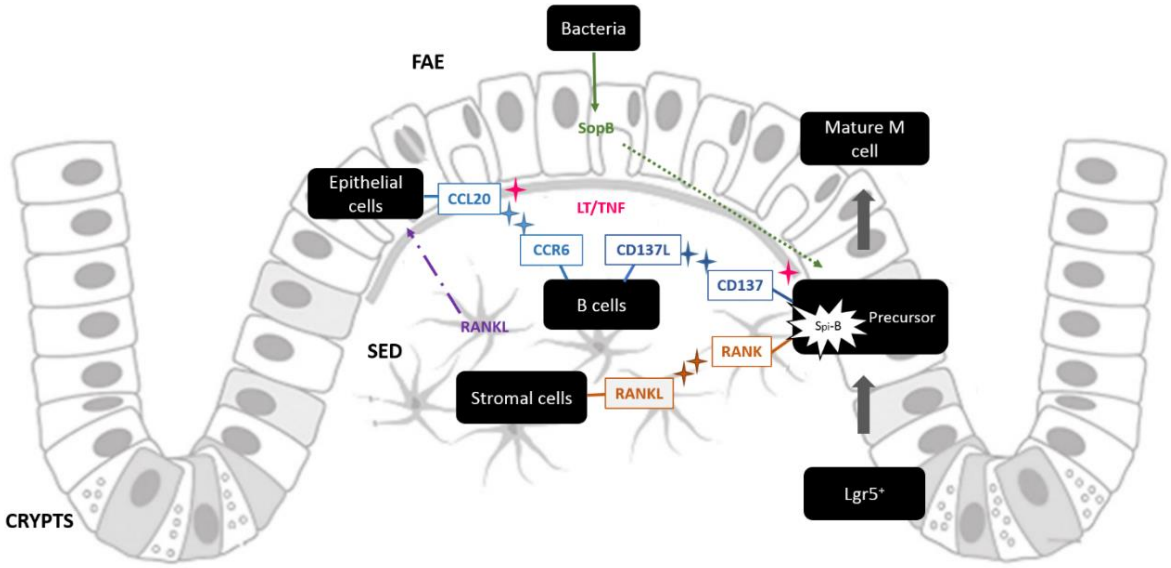

Figure 3 - Representation of the possible mechanisms behind M cell genesis. Lgr5$^+$ differentiate into FAE cells precursors, including M cells precursors. Stromal cells produce RANKL, which is thought to be bound to the cell surface or in soluble form dispersed in SED, and the cytokine will interact with RANK at the precursor cells surface. This interaction will induce Spi-B expression that could induce the maturation into functional M cell. Immune cells can also induce M cell phenotype. These cells are attracted to the dome region by the cytokine CCL20 produced by epithelial cells. The latter phenomena could be a response to RANKL stimulation, or by action of lymphotoxins. Immune cells interact with CCL20 through their receptor CCR6 and also interact with M cell precursors through the interaction CD37L-CD37, which seems to induce M cell maturation. Once again CD137 expression could be induced by lymphotoxins. Another external factors can induce M cell maturation which is the case of SopB produced by bacteria that will stimulate molecular pathways in the M cell precursors (one of them is thought to be RANKL – Spi-B differentiation pathway).

The referred study of *Tahoun et al* intended to determine if the infection agents, namely *S.Typhimurium,* could either trigger transdifferentiation of epithelial cells into M cells or induce *de novo* genesis of M cells. The experiment led to an increase in M cell numbers and interestingly it seemed result of the release of the cytokine RANKL[62]. The study revealed that the bacteria secreted an effector protein, SopB, which is known for controlling many cellular pathways during different stages of infection[63-65], into host cells and acted as the mediator of M cells RANKL-dependent differentiation[62]. It is described that RANKL-RANK activation prompted expression of Spi-B and also the epithelial–mesenchymal transition-regulating transcription factor Slug that induced the FAE enterocytes to differentiate into M cells. Another report about M cell differentiation induced by bacteria infection brings up again a possible role of the immune cells and comes from the hypothesis that the cytokine macrophage migration inhibitory factor (MIF) was produced rapidly after *in vivo* bacterial challenge, by CD11c$^+$ cells located beneath the FAE of PP, and also had the capacity to induce the appearance of M cell –like features[66].

On Figure 3 there is a schematized summary of the molecules and interactions which were previously referred as mechanisms underlying M cell genesis. Whether or not M cells precursors have their phenotype defined, it seems that signals somehow associated with B cells are necessary to complete M cells maturation. So, it is reasonable to consider that M cell development might be a process in steps in which the first lineage commitment step is B cell independent, and is followed by a step that is dependent on B cells or other external factors. Nevertheless, there is not a decisive genesis model, or at least not one that could put together all interesting points that the different theories present. More experiments are still needed in order to clarify the differentiation process and the role of molecules such as CCL20, CD137, RANKL, Spi-B, SopB, LT.

2.2.3. M cells in other MALT

The morphology of M cells in GALT have been thoroughly studied, but relatively little is known about the presence and properties of M cells in MALT outside the gut. Such tissues can be found in the oropharynx, along the upper and lower airways, in the salivary gland ducts, among others[7]. Thus it should be expected to find a cell type similar to intestinal M cells in their associated epithelium to perform antigen sampling.

The oro- and nasopharynx lymphoid tissue, which is called the Waldeyer's ring in humans, is formed by the palatine, pharyngeal, lingual and tubal tonsils[67]. Along with the lymphoid tissue of the nasal cavity, these tissues constitute the nasopharyngeal associated lymphoid tissue (NALT)[68,69], although some authors refer to them separately[70].

There are different types of epithelium covering the tonsils: the palatine and lingual tonsils are covered by a squamous stratified epithelium, and the pharyngeal and tubal tonsils are covered by a respiratory epithelium[7].

Structural and histochemical features of M cells present in the epithelial cells of tonsils have been described in some animal models: irregular microfolds, the ability to take up tracers, the presence of the cell marker vimentin (in the case of rabbit's tonsils), close contact with intraepithelial lymphocytes[7,61], and a specialized composition of glycoconjugates in their apical membrane which could be involved in the adhesion and uptake of inhaled or ingested particles[71]. For some time, studies failed to detect a separate epithelial cell type in human tonsils, but nowadays specific human tonsillar M cell markers, such as class II b-tubulin, are identified. The basic structure of M cells in the human nasopharyngeal lymphoid follicles is the same as in the PP. Thus, it is likely that the M cells in nasopharyngeal lymphoid follicles of the Waldeyer's ring are sites of antigen uptake for induction of mucosal immunity[68].

On the other hand, a study demonstrated that specific immune responses were induced by infection via the upper respiratory tract on mice with structural and functional defects of NALT, suggesting that additional inductive sites and/or M cells are present in that region[72]. The authors identified M cells developed in the murine nasal epithelium as an alternative and NALT-independent gateway for the sampling of respiratory antigens. However, differences between murine and human epithelium points that the presence of respiratory M cells in the nasal cavity might be a unique feature of the mouse[72].

It is described that the induction of the M cell phenotype in the case of NALT M cells is as complex as it is for the intestinal cells. Instead of a rapid turnover and crypt stem cell origin, airway epithelial cells are generated from a dispersed population of basal cells and have half-lives on the order of weeks to months[73]. Regardless of their different origin and turnover mechanism, NALT and GALT M cells show very similar phenotype and functions, indicating that convergent or overlapping genetic programs are induced[56].

While bronchus-associated lymphoid tissue (BALT) is found in rats and rabbits, it is present only rarely in healthy adult humans[7]. Likewise its development seems to be related to microbial stimulation and can be induced by infections and vaccinations[74].

The lymphoepithelium that overlies the lymphoid tissue of the bronchi differs in several aspects from the ordinary respiratory epithelium. The number of ciliated cells is reduced, goblet cells are rare, but numerous lymphocytes and also some macrophages lie among the epithelial cells[7]. Similarly to other MALT, M cells were found among other epithelial cells of the dome area of BALT in rabbits. It was also shown that antigen and viruses were transported more avidly by M cells than by other epithelial cells. Still, no M cells have been evidently characterized for BALT in humans[7,75]. *Toyoshima et al* reported BALT induction after exposure of the airways of mice by *P. aeruginosa*, with higher response as well[76]. Moreover, M cells in the lung have also been recognised as entry sites for *Mycobacterium tuberculosis* in mice[77].

2.3. In vitro intestinal cell models

Intestinal *in vitro* models have been established in order to evaluate the intestinal absorption of drug candidates. *In vitro* models are cheaper and less laborious when compared to *in vivo* techniques. Also, they replace and reduce the use of experiments with animals, valuing the 3R's policy[78]. On the other hand, one cannot extrapolate the data to the *in vivo* situation since these models do not consider physiological factors that influence absorption such as GI pH, intestinal emptying rate, control by the nervous system and systemic blood flow[79,80].

2.3.1. Caco-2 monoculture

Caco-2 cells are an immortal human cell line derived from a human colorectal adenocarcinoma. In culture they grow into a confluent monolayer, differentiate and behave similarly to enterocytes, in terms of function and structure, resembling normal intestinal epithelium[81]. It is the most used cell model to study the permeability of drugs over the last 20 years, and is accepted as standard assay to predict drug intestinal permeability in humans by pharmaceutical companies and controlling authorities[82]. When Caco-2 cells are grown in a semipermeable membrane, the apical compartment corresponds to the intestinal lumen and the basolateral compartment corresponds to the serosal side, simulating the vivo intestine[83,84].

The cell differentiation starts when the cells achieve confluence, around 7 days, and is completed within 21 days. That is when the cells are polarized and connected to each other through tight junctions (TJ), exhibiting an apical brush border structure with several enzymes, membranar active, ionic and non-ionic transporters and receptors[16].

Nevertheless, this system presents some shortcomings, namely the overexpression of P-glycoprotein, an efflux pump, when compared to primary small intestinal enterocytes, and the fact that these cells form tighter junctions than those found in the human epithelium, which could lead to decrease the paracellular permeability[85]. Additionally, the Caco-2 monoculture does not contemplate some other important factors that influence the functionality of enterocytes such as the mucus layer or the interactions between the epithelium and the stroma[86]. Furthermore, in another perspective, the referred cell culture process requires about 3 weeks which is labor intensive and time consuming, limiting its wide application in high-throughput screening of a large number of compounds[87].

2.3.1.1. Accelerated Caco-2 models

With the aim of shortening and simplify the process of Caco-2 cell culture, some modified Caco-2 culture protocols have been reported in which a minor period of culture time is required. *Lentz et al*. have developed a more rapid, reduced serum culture system for Caco-2 monoculture, in which iron and a combination of growth factor and hormones were added to the culture media[88]. However the effects of these individual substances on Caco-2 cellular growth are unclear[87]. *Chong et al* used a BioCoat® Intestinal Epithelial Cell Environment claiming that it resulted in a Caco-2 monolayer suitable to be an absorption model in only 3 days[89]. However, these procedures typically only reduce the time required to obtain monolayers ready for transport studies with up to 3 days. Also, Caco-2 cells grown in these conditions may not develop tight junctions or express fewer efflux pumps, which limit the utility of such models[90].

Another study, from *Sevin et al*, reports an evaluation of an accelerated 6 days Caco-2 cell permeability model obtained by using puromycin treatment of the cells. Strong correlations were obtained between the apparent permeability of the drugs in the accelerated model and in the traditional models and comparable efflux ratios were observed in the both models[90].

A report from BD-BioSciences describes another decreased time model that revealed results of a Caco-2 monolayer after only 3 days, by using a three-dimensional extra cellular matrix substrate and an optimized serum-free medium[91]. In this experiment it was used Differentiation Medium (containing butyric acid serum-free DMEM with MITO+™), which was also used in *Cai et al* experiments on a 7 days Caco-2 model that displayed comparable cellular morphology and integrity with the traditional 21-day model and no significant differences in paracellular and transcellular permeability[87].

Peng et al indicated similar results regarding permeability values and efflux ratios between a 7 days model and the established 21 days model. The cells were seeded the in collagen coated transwells[92]. A coating procedure was also transversal to the two previous mentioned studies.

Nevertheless, multiple protocols for the culture of Caco-2 cellular models result in diverse cellular morphology and transporter expression[88], so it is difficult to establish a new protocol that requires less time to develop a suitable and reliable Caco-2 intestinal model.

2.3.2. Caco-2:Raji B co-culture

As M cells constitute a minor subset of intestinal epithelial cells in the FAE and are difficult to isolate, study of the signaling involved in their development and maintenance is quite complex. Several approaches are used to investigate these cells and one is the use of an in vitro model of M-cell differentiation. As it was mentioned on section 1.2.2., it was reported that Raji B cells, a cell line that is originated from a human Burkitt's linfoma, induce M cell's phenotype in Caco-2 cells.

Kérneis established an *in vitro* model to study the properties of M cells by settling a co-culture of Caco-2 cells with lymphocytes isolated from mouse Peyer's patches that were added at the 15th day of the culture. After a couple of days of direct contact it was possible to observe accumulation of lymphocytes in intraepithelial pockets, as do M cells in vivo[45].

Later, Gullberg and co-workers developed a new co-culture system in which, Caco-2 cells were seeded on normal oriented inserts and after 14 days human Raji B lymphocytes, were added to the basolateral chamber of the Transwell™ [93]. This means that lymphocytes were not in direct contact with Caco-2 cells, although it resembles better the physiological conditions. In this system it was possible to observe that some cells developed M-cell like morphology.

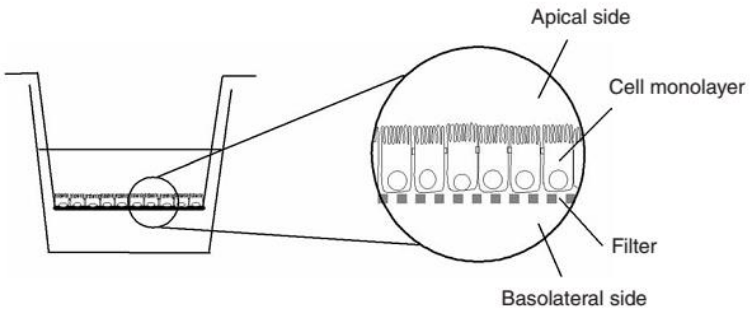

Figure 4 - Schematic representation of the co-culture model on a Transwell. Caco-2 cells are seeded on the Transwell membrane while Raji B are added later to the basolateral compartment. Image adapted from *Hubatsch et al*, 2007[118]

Afterwards, the effect of M cells on the transport of drugs in comparison with the Caco -2 cell model was studied by Rieux's group, this time using Gullberg's model. It was assessed the transport of nanoparticles versus the drug in the free form and the group described that M cells increased the transport of the encapsulated drug[94], indicating that these cells participate in the transport of nanoparticles.

Although the Caco-2:Raji B model still lacks the influence of mucus and stromal cells, it mimics the uptake of particles in a more reliable way. It is also a great tool to explore the differentiation of enterocytes into M cells and inherently it is a way to discover the interactions between epithelial cells and lymphocytes.

- This page was intentionally left blank. -

Chapter 3

Aim of the project

The project here presented is included in the overall aim to develop an intestinal cell-based engineering model to study the absorption of nanoparticles containing biopharmaceutical drugs. More particularly, this thesis was developed within the context of the enhancement of the Caco-2:Raji B co-culture model, by optimizing the conversion of Caco-2 cells into M cells in a similar extension to the *in vivo* tissue. For that, the transdifferentiation process and the molecular factors responsible for the phenotypic shift must be studied. Additionally to this goal, a new improvement to the intestinal in vitro cell models was proposed: the study of M cells in a more rapid and cheaper manner. This proposal was based on the hypothesis that induction of M cell phenotype would also work in an early time of Caco-2 cell maturation, since it is a process that somehow requires a certain phenotypic plasticity.

Thus, the final aim is to assess a 7-days co-culture model as a suitable tool for the study of *in vitro* M cell transdifferentiation, which would have an enormous positive impact in the development of intestinal cell models by sparing time and money.

To do so, the first objective is to validate the model in comparison with the 21-days model in terms of development of Caco-2 cells. This implies the evaluation of certain parameters: the integrity of the cell monolayer, the expression of certain cell markers, the enzymatic activity of brush border enzymes and the ability to transport substances. Then, one should compare the two models in the co-culture system where some cells should differentiate into M cells, causing changes on the previous mentioned parameters.

A such, there will be four systems to analyse: 7-days Caco-2 monoculture, 7-days Caco-2:Raji B co-culture, 21-days Caco-2 monoculture, 21-days Caco-2:Raji B co-culture.

- This page was intentionally left blank. -

Chapter 4

Materials and Methods

4.1. Establishment of the co-culture system

4.1.1. Cell culture and subculturing

Caco-2 cell line was obtained from American Type Culture Collection (ATCC). Raji B cell line was kindly provided by Dr. Alexandre Carmo from Cellular and Molecular Biology Institute (IBMC), Porto, Portugal. Caco-2 cells were used between passage numbers 22 and 40 and Raji B cells between 30 and 42.

Both cell lines were cultured and grown separately in tissue culture flasks (Orange Scientific) in a complete medium, consisting of DMEM (Dulbecco's Modified Eagle's medium) supplemented with 10% (v/v) heat-inactivated Fetal Bovine Serum (FBS), 1% (v/v) L-glutamine, 1% (v/v) non-essential amino acids and 1%(v/v) penicillin/streptomycin. Unless otherwise stated, all reagents regarding cell culture were purchased from Gibco (Invitrogen Corporation, Life Technologies). Cells were maintained at 37°C in a humidified atmosphere of 5% CO2. Medium was changed every two or three days, and cells were regularly sub-cultured when reaching 70-80% of confluence as follows. Medium was removed, cells were washed with sterile Phosphate Buffered Saline (PBS, pH 7.4: 147 mM NaCl, 2.7 mM KCl, 1 mM CaCl2, 0.5 mM KH2PO4, 3.2 mM Na2HPO4 and 5.5 mM glucose). To detach them it was used a 0.25% (w/v) Trypsin-EDTA solution for 5-10 minutes at 37°C that was then inactivated by the addition of double volume of complete medium. A small aliquot of the cell ressuspension was then mixed with 0.4% (v/v) trypan blue (Sigma) and cell were counted using a Neubauer chamber. Cell density was determined by the trypan blue exclusion test of viability:

$$\text{No. cells/ml} = \frac{Total\ viable\ cells\ number}{no.of\ squares} \times dilution\ factor \times 10^4$$

A volume of cell suspension was transferred to new T75 culturing flasks, with 10 mL of fresh complete medium, corresponding to a cell density of 6 to $8x10^5$ cells/flask and 1 to $2x10^6$ cells/flask for Caco-2 cells and Raji B cells, respectively. As Raji B cells are in suspension the trypsinization step is skipped and the following steps were maintained. Every time PBS or complete medium was added to the cells the solutions were pre-warmed at 37°C.

4.1.2. Cell seeding

For all experiments cells were cultured on 24-well culture plates (Corning). Caco-2 cells were seeded at a cell density of $1x10^5$ cells/cm^2 and a number of Raji B cells corresponding to twice the number of Caco-2 cells was then added to the system. Depending on the experiment two different set-ups were used.

To perform the permeability studies, the evaluation of the monolayer integrity and the assessment of the morphology by Scanning Electron Microscopy (SEM) and Transmission Electron Microscopy (TEM), the cells were cultured in the Transwell system of polyethylene terephthalate transwell (BD Falcon™) with 8 µm size pores. In this set-up, Caco-2 cells were seeded on the apical side of the insert, which was filled with 300 µL of complete medium, and the Raji B cells were added to the basolateral chamber, which was filled with 800 µL, at day 15-18 for the 21-days model or at day 3 of the 7-days model. This experimental set-up is represented on figure 4. Medium was change every 3 days and after the addition of Raji B cells only half of the volume was removed and replaced by fresh medium.

To perform the alkaline phosphatase assay cells were seeded directly on the culture plate and to perform immunofluorescence staining cells were seeded on top of coverslips to facilitate image acquisition. The seeding conditions were the same as in the previous set-up, except Caco-2 and Raji B cells were in direct contact and the total volume of complete medium was around 1mL.

In all experiments of the 7 days-model, the inserts/coverslips/culture plate were coated with rat tail collagen type I just before the Caco-2 cell seeding, in an attempt to induce a more rapid development of the model, since it was described that fibrillar collagen accelerates the development of a tight monolayer by Caco-2 cells[91].

All the experiments, except for the samples for morphological analysis, were performed in triplicates.

4.1.3. Collagen type I coating

For the 7-days culture, before cell seeding, it was performed a coating of with Collagen I from rat tail tendons (Gibco®, Invitrogen) and manufacturer's instructions were followed. Firstly, the collagen stocking solution of 3 mg/mL was diluted to 50 µg/mL in 0.02 M acetic acid. Then, the solution was added to the Transwells/coverslips at 5 µg per cm^2, incubating at room temperature. After 1 hour, the solution was aspirated and the surfaces were rinsed three times with equal volume of PBS to remove de acid. The cell seeding happened immediately after.

4.2. Assessment of the monolayer integrity

4.2.1. Measurement of Transepithelial Electrical Resistance

The evaluation of the epithelial integrity was made by measuring the transepithelial electrical resistance (TEER). The measurements were made every three days and during the permeability assays, using an Electric-Volt-Ohm Meter device from Millipore®. TEER increases with culture time, reaching a plateau value after about 10 days, when the adhesion between the cells should be already formed[95].

Before every measurement, the electrodes were equilibrated with culture medium for 3-5 minutes. The computed values were obtained by deducting the resistance values of the insert filter and the culture medium and multiplying it by the surface area of the Transwell.

4.2.2. Assessment of Paracellular Permeability

Permeation studies were performed using 4kD Fluorescein isothiocyanate–dextran (FITC-dextran, Sigma-Aldrich) - a fluorescent marker for paracellular transport - which can indicate the integrity of the membrane. After cell-washing and equilibration in PBS, 300 µL of FITC-dextran solution at a concentration of 200µg/ml were added to the apical chamber, while 800 µL of PBS were added to the basolateral chamber. The assay lasted 2 hours and every 15 minutes 100µL were taken from the basolateral chamber to a black micro-assay 96-well plate (Greiner Bio-one) and substituted with 100µL of PBS. In the last time-point 100 µL were also recovered from the apical chamber. The plates were maintained at 37ºC with an agitation of 80 RPM during the course of the experiment. TEER measurements were also performed every 30 minutes during the assay to assess membrane viability.

4.2.2.1. Fluorimetry

The collected samples from the paracellular permeability assay were analysed by fluorimetry. A calibration curve was obtained by using solutions with known concentrations of FITC-dextran) from which the concentration values of the samples were extrapolated. Fluorescence was read using a Synergy™ Mx HM550 microplate reader (BioTeK® Instruments) at an emission wavelength of 520nm and excitation wavelength of 495nm. Microplate readings were obtained through Gen5 Data Analysis software (BioTek® Instruments). The apparent permeability (P_{app}) was calculated with resource to the calibration curve, by calculating the mass of FITC-dextran in each sample and using the following equation:

$$P_{app} = \frac{\Delta Q}{A \times C_0 \times \Delta t} \ ,$$

where C_0 is the initial concentration in the apical compartment (µg/mL), A is the surface area of the insert (cm^2), Δt is the time correspondent to the time-point (seconds) and ΔQ is the concentration of compound detected in the basolateral side (µg/mL).

4.3. Permeability study

After cell-washing and equilibration in PBS, 300 µL of insulin solution at a concentration of 100 µg/mL were added to the apical chamber, while 800 µL of PBS were added to the basolateral chamber. The assay lasted 4 hours and at the time-points: 15 min, 30 min, 1h, 2h, 3h and 4h, 100µL were taken from the basolateral chamber to a black micro-assay 96-well plate (Greiner Bio-one) and substituted with 100µL of PBS. In the last time-point 100 µL were also recovered from the apical chamber. The plates were maintained at 37ºC with an agitation of 80 RPM during the course of the experiment. TEER measurements were also performed every time a sample was taken to assess membrane viability.

Complementary studies to integrity were performed at the end of permeability studies to evaluate the final integrity state of the monolayers. For this, apical-basolateral flux was assessed using 4 kDa FITC-Dextran which occurred the same way as described on the previous section but with only one time-point taken after 1 hour.

4.3.1. Insulin quantification

The samples were further quantified by reverse HPLC-UV on a Merck-Hitachi LaChrom HPLC instrument (Merck). The HPLC system was equipped with a XTerra RP-18 column, 5 µm particle size, 4.6 mm internal diameter × 250 mm length (Waters) and a LiChrospher 100 TP-18, 5 µm particle size guard column (Merck). The experiment was run at room temperature and the total

area of the peak was used to quantify insulin[96]. The results were expressed in percentage of release and apparent permeability (Papp), calculated as presented on section 2.3.2.

4.4. Morphological and structural characterization

4.4.1. Scanning Electron Microscopy (SEM)

Transwell membranes were first washed twice in PBS, following primary fixation with 3% (v/v) Glutaraldehyde (AGAR Scientific) in 0.1M sodium cacodylate during 45 minutes at room temperature. After rinsing with 0.1M sodium-cacodylate buffer (Fluka®), membranes were incubated with secondary fixative 1% (v/v) osmium tetroxide in 0.1M sodium cacodylate buffer for 1 hour at 4°C. Membranes were washed with 0.1M sodium-cacodylate buffer, following dehydration through a graded series of ethanol for 10 minutes each. To dry the membranes it was used (HMDS, Sigma) solution to incubation for 10 minutes and then the samples were air-dried. Finally, the membranes were removed from the transwell insert with a scalpel blade and placed on the top of double-sided sticky tape that was placed on top of an aluminium stub. Before observation the samples were sputter coated with 200 Angstroms of Gold-Palladium. Images were acquired using Quanta 400FEG ESEM/EDAX Genesis X4M.

4.4.2. Transmission Electron Microscopy (TEM)

Transwell membranes were first washed twice in PBS, following primary fixation with 2.5% (v/v) Glutaraldehyde (AGAR Scientific) in 0.1M sodium cacodylate during 3 days at 4°C. After rinsing with 0.1M sodium-cacodylate buffer, membranes were post-fixed in 2% (v/v) osmium in 0.1M sodium cacodylate buffer overnight. Membranes were washed with 0.1M sodium-cacodylate buffer, following dehydration through a graded series of ethanol and propylene oxide for 10 minutes each. The membrane was infiltrated in embedding resin as follows: propylene oxide and epon (2:1 proportion), 1:1, 1:2 and 0:1 during 1 hour each. After that, resin was allowed to harden during 48 hours in an incubator set at 65°C. The block was sectioned with 60 nm of thickness using a Leica Reichert SuperNova ultramicrotome (Leica Microsystems) and samples are collected to an aluminium disk. The disks were contrasted using uranyl acetate and lead citrate during 5 minutes in each solution. Images were acquired using a transmission electron microscope Jeol JEM 1400.

4.4.3. Immunofluorescence staining

The staining procedure were performed entirely on the coverslip containing the Caco-2 cells monolayer. Generally, all of the presented immunofluorescence staining procedures are composed by some key steps: fixation, permeabilization (if required), blocking, incubation with primary antibody, incubation with secondary antibody (if applicable) and mounting. Between these steps there are washing steps that consist in washing the cells three time with PBS for 5 minutes. Every time a washing step is mentioned it consists on the previously described.

In all the immunofluorescence staining practices two fixatives were tested: 2% (v/v) paraformaldehyde (PFA, Merk) solution and methanol (Sigma). Regarding the first mentioned fixative, cells were incubated with PFA for 15 minutes at room temperature, followed by a washing step to remove the fixative; then the next step comprised a permeabilization procedure with the incubation for 7 minutes with a 0.05% Triton X-100 (Sigma) solution also at room temperature. The alternative method was to perform the first washing step with cold PBS and then incubate the cells for 10 minutes on ice with cold methanol. After this step, cells were washed again for the removal of the fixating agent and no permeabilization step was necessary. After this, cells were incubated in blocking solution – PBS + 10% (v/v) Fetal Bovine Serum (FBS) - for 30 minutes at room temperature, so that the antibodies would not bind non-specifically in the next step. Then, without washing, the blocking solution was removed and the cells were incubated with the primary antibody solution. In the case of Alkaline Phosphatase the staining was obtained by incubating the cells with intestinal alkaline phosphatase rabbit polyclonal antibody (Biorbyt) at a dilution rate of 1:100 in PBS, for 1 hour at room temperature. The staining of Galectin-9 was obtained by incubating the cells with purified galectin-9 mouse anti-human antibody (BioLegend) at a dilution rate of 1:50 in PBS, overnight at room temperature in a humidified chamber. Occludin was stained through the incubation with occludin mouse monoclonal antibody-Alexa Fluor® 594 (Invitrogen) at a dilution rate of 1:100 in PBS for 1 hour at room temperature. After washing cells previously incubated with anti-Alkaline phosphatase antibody and anti-galectin-9 antibody were incubated with the secondary antibodies Alexa Fluor®594 Goat Anti-rabbit (Invitrogen) and Alexa Fluor®594 Rabbit Anti-Mouse (Invitrogen), respectively, at a dilution rate of 1:1000 in PBS, for 1 hour at room temperature, protected from light. Finally, were washed again and were incubated with 4',6-diamidino-2-phenylindole (DAPI, Sigma Aldrich) for nuclei staining for 10 minutes and mounted in Fluoromount™ Aqueous Mounting Medium (Sigma Aldrich). Inverted Fluorescence Microscopy images were obtained using a Zeiss (Germany) Axiovert 200M inverted fluorescence microscope and analysed using AxioVs40 v4.8.2.0 software.

4.5. Enzymatic Activity Assessment

4.5.1. Alkaline phosphatase activity assay

The assessment of alkaline phosphatase was evaluated as it is an indicator of Caco-2 cells differentiation. Culture medium was removed from the wells and cell monolayer washed twice with PBS. Then, 1 ml of reaction buffer was added to the wells. This reaction buffer was composed by 1 volume of collection buffer (10 mM Tris–HCl, 150 mM NaCl) and three volumes of p-Nitrophenyl phosphate (p-NPP) solution. This last solution was composed by 2.5 mg/ml p-NPP (Sigma-Aldrich) dissolved in 100 mM diethanolamine (Sigma-Aldrich), 150 mM NaCl and 2 mM MgCl2. The assay occurred for 12 minutes at 37ºC with an agitation of 80 RPM. Samples of 100 µL were collected every 2 minutes and transferred to a black micro-assay 96-well plate (Greiner Bio-one) which wells contained 50 µL of 0.5 M NaOH to stop the reaction. The standard curve was prepared with 50 µL of each p-Nitrophenol (p-NP) standard solution (Sigma-Aldrich) (concentration range: 0–600µM) added to 150µl of pNPP solution and 50µl of 0.5 M NaOH. Absorbance was read in Synergy™ Mx HM550 microplate reader (BioTeK® Instruments), at 405 nm, and converted to concentration after blank subtraction with reference to the standard curve and corrected for the reaction volume. Then the concentration values were plotted as a function of time. Finally, enzyme activity was calculated from the angular coefficient of the linear slope and expressed as mU = nmol of p-NP/min and normalised to mg of cellular protein. Quantification of cellular protein was performed accordingly to the Lowry method[97], using the DC Protein Assay (Bio-Rad).

4.6. Statistical analysis

Statistical analysis was performed using GraphPad Prism 5 software. Mean and standard deviation were calculated for each sample. A one-way analysis of variance (ANOVA) with Tuckey post test was used to evaluate group's comparison. Samples were considered significantly different if a difference of $P < 0.05$.

- This page was intentionally left blank. -

Chapter 5

Results and Discussion

The principal objective of this project is to assess the 7-days model characteristics and its validity as a tool to study M cells differentiation. As such, the effects of the different culture periods will be assessed and the differences between the co-culture and monoculture will be analysed as well.

As it was mentioned before, the study subjects consist in 4 different models: Caco-2 monocultures with culture time of 7 days and of 21 days, and Caco-2:Raji B co-cultures with 7 days and 21 days of culture time as well. In every following section, the data regarding each model will be compared and analysed.

5.1. Comparison of the monolayer integrity

5.1.1. Assessment of Transepithelial Electrical Resistance

The first step of the project was to evaluate the integrity of the cell monolayer in the four conditions above mentioned. Since the integrity and robustness of the cell monolayer is dictated by the presence and graduate stronger tight junctions between cells[95], it is expected that the time in culture will influence the transepithelial electrical resistance. The following graphs contain the TEER values obtained for the models.

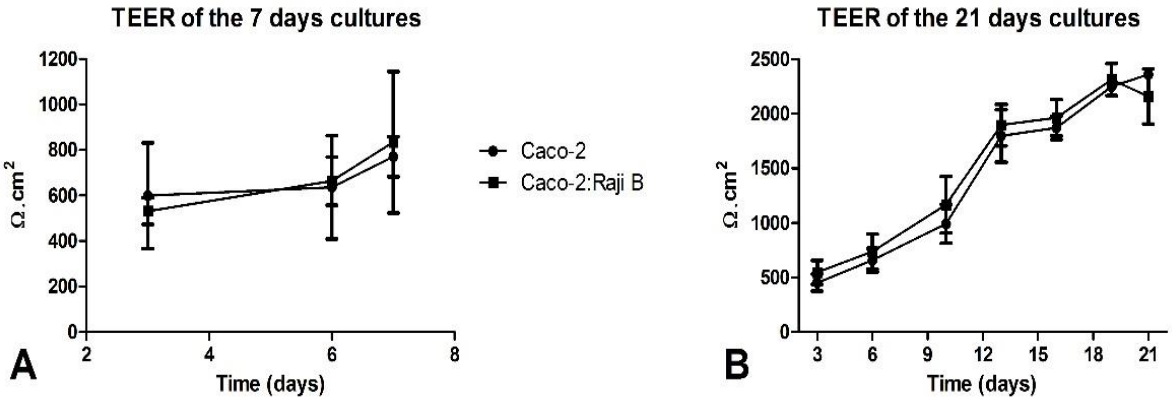

Figure 5 – Evolution of the TEER along the culture time in the different cell models. On A are presented the TEER values for the monoculture and co-culture of 7 days; on B are presented the TEER values for monoculture and co-culture of 21 days.

In fact, on figure 5 it is observable that the TEER, increased with culture time in all models as expected. In the literature is described that TEER of Caco-2 monolayers reach a maximum after about 10-15 days[95]. In the 21-days cultures, although there was a slight increase of the TEER in the last days, it was verified that the after 12 days in culture a plateau was reached, so in this aspect there is concordance with the literature. However, there is disagreement in what concerns the TEER values. As one can easily visualize on figures 5 and 6, the highest TEER value obtained for the 21-days culture is somewhere between 2000 to 2500 ohms.cm^2, and the reported range of such values is between 150 to 1600 ohms.cm^2 [95,98]. Though the obtained values are fair above of what was expected, the reference consists in a broad range of values which leads to conclude that there is some accepted variability in this parameter, as it depends on the numbers of cells seeded, filter support, culture condition, and passage number[95,98].

Figure 6 reveals that once more as it was expected, the TEER values obtained for the 7-days cultures were significantly lower than the 21-days cultures values. Even though the cells were seeded on collagen fibers, TEER depends highly on the tightness of the junctions between cells and these take some time to fully develop[99]. So, although the monolayer of the 7-days model may be intact, the TJ between the cells are not as tight as in the 21-days model, so the proposed model fails in this parameter. Still, the implications of this failure have to be ponder.

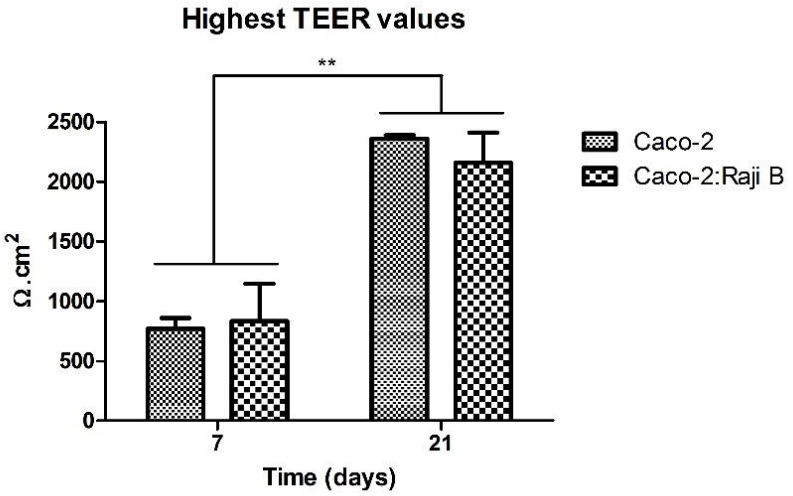

Figure 6 - Highest TEER values obtained for the 7 and 21 days monocultures and co-cultures. The difference between the 7-days model and the 21-days model TEER is statistically significant ($p<0,05$). However, there is no significant statistically difference between the TEER of the monocultures and the co-cultures ($p>0,05$).

The results of other parameters assessment must be analysed to make a correct assumption of the implications of the lower TEER values of the model.

Concerning the effects of the presence of the Raji B cells in the co-cultures models, as it is evident on both of the previous graphs, there is no significant difference between the TEER values of the monoculture and the co-culture systems in both 7 and 21-days models. It would be expected that he presence of Raji B cells in the co-culture models could have an impact on the integrity of the cell monolayer. In fact it was described that in such cell model TEER values obtained in the co-culture were lower, due to the transformation of enterocytes in cells with M-phenotype which do not form TJ as tight as in the Caco-2 monocultures[35]. The obtained results mean that if the conversion of Caco-2 cells into M cells happened, two of the follow events took place: either the process was not relevant enough to cause loss of the junctions tightness between a significant group of cells, or the transdifferentiation did not affect this parameter.

5.1.2. Paracellular permeability assessment

Another way of assessing the integrity of the monolayer was accomplished by determining the paracellular permeability to hydrophilic tracers which can be monitored with compounds that are labelled fluorescently, such as dextrans. So, in order to do so, the permeability of

FITC-dextran was determined and also TEER, whose first time point was obtained after the substitution of DMEM for PBS, was measured during the assay, as it is presented on figure 7.

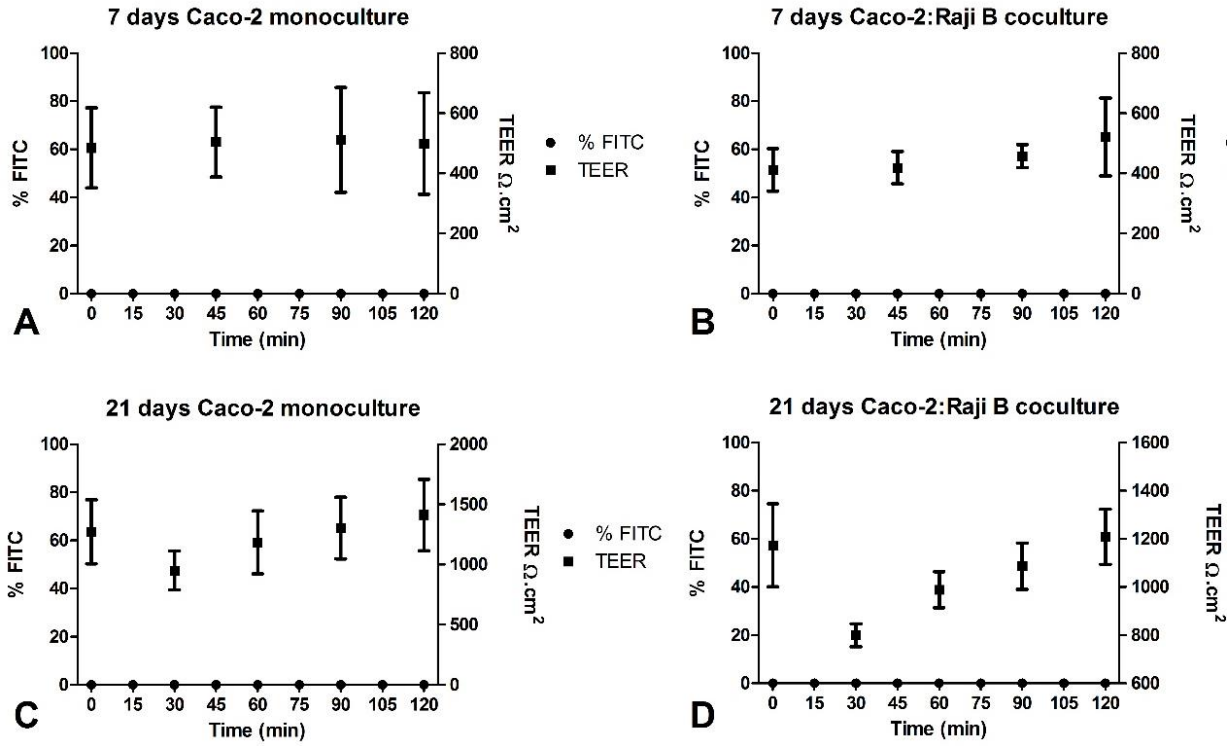

Figure 7 - Permeation and TEER profiles during the permeability assay with FITC-dextran of different cell models. The dots represent the percentage of FITC and the squares represent the TEER values. A - Permeation profile of the 7-days Caco-2 monoculture; B – Permeation profile of the 7-days Caco-2:Raji B co-culture; C – Permeation profile of the 21-days Caco-2 monoculture; D – Permeation profile of the 21-days Caco-2:Raji B co-culture.

In the previous graphs it is visible that none of the cell models was permeable to FITC dextran. There was no detectable compound on the basolateral side of the Transwell during the whole assay meaning that all the FITC-dextran was retained by the cell monolayer. It is also observable that all the systems maintained high TEER values throughout the permeability study. As it was expected, the 7-days models TEER values were lower when compared to the 21-days model values, but the measurements were practically stagnant with time. The 30 minutes measurement on the 21-days co-culture assay (D) was an exception, but it was likely due to an abnormal reading, explaining the following increase of TEER values.

Such results reveal that not only cell monolayers were intact, but also the tight junctions between cells were narrowly and strongly tight. Although reported permeation studies indicate that TEER values usually decrease, representing the increase of permeability through the TJ [100], the obtained results are valid as long the cell barrier is perfectly intact. The described pore

radius of Caco-2 cell tight junctions is around 4,5 Å[101] and the approximate Stokes radius of the 4 kDa FITC dextran is around 14 Å[102].

This outcome is particularly interesting when judging the ability of the 7-days model to work as an epithelial cell barrier. The absence of permeability of the 7-days models is in consensus with the fact that it takes only around 4 days until the tight junctions of the Caco-2 cell monolayer are detected[103], so as long they are intact, 7 days should be enough to create a cell barrier. Thus, justification for differences in TEER values between the 7 and 21-days models is still not explained. In fact, tight junctions include a series of transmembrane proteins, which form fibrils that cross the plasma membrane and interact with proteins in the adjoining cells[104]. The transmembrane proteins interact with the actin cytoskeleton within the cell through proteins[99]. So, it is reasonable to accept that at the 7th day tight junctions might be at a development stage where the pore size is sufficient to prevent the paracellular passage of hydrophilic compounds such as FITC dextran, but the associated cell machinery may not be fully developed for the selective regulation of the paracellular passage of ions, explaining the lower TEER values.

When comparing the monocultures with the co-cultures, once again there is no observable difference. There was not an increase in the paracellular permeability that could be explained by the fact that M cells form less tight junctions, allowing the passage of the FITC dextran[35]. So, either the transformation did not happen or it happened at an extension that is non-detectable by this parameter.

Nevertheless, and summing up the positive outcomes of this section, although TEER values are lower, the 7-days model seems to be as suitable as the traditional model when it comes to the integrity of the cell monolayer.

5.2. Permeability studies

The following permeation study aimed to test cell models ability to work as a functional epithelial physiological barrier. It was described that the presence of M cells in the co-culture system resulted in higher uptake/rate of transport of particles[35,105], so this aspect will be analysed when comparing the monoculture versus the co-culture systems.

5.2.1. Insulin Permeability Studies

In order to assess the capability of the new models to be a tool for drug permeability studies, insulin transport studies were conducted. Also, in the end of the assay, in order to assess monolayer integrity, it was performed a paracellular permeability assay with FITC-dextran, for 1 hour. The following graphs contain the permeability profiles for insulin.

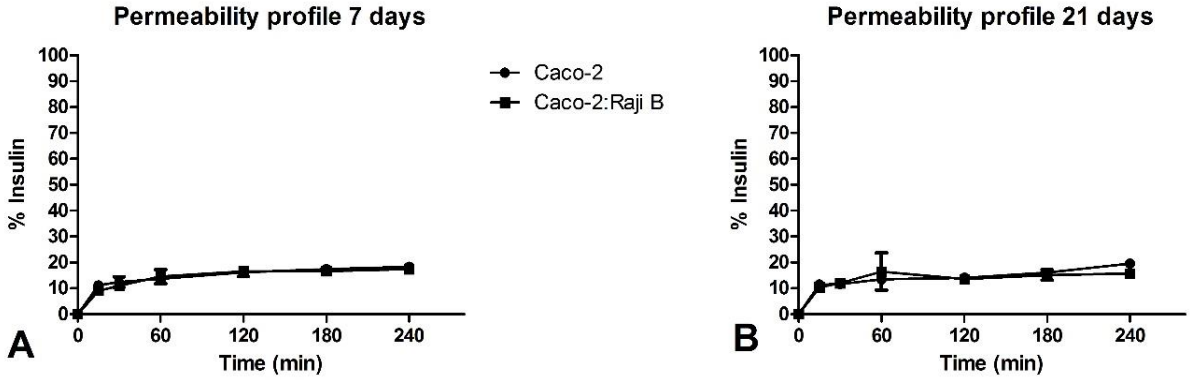

Figure 8 – Cumulative permeation profile of the models for the insulin permeability assay. On A: permeation profile of the 7 days mono and co-cultures. On B: permeation profile of the 21-days mono and co-cultures. On the vertical axis is represented the percentage of the insulin that crossed the cell monolayer to the basolateral side throughout the time (horizontal axis) of the assay. There are no significant differences between the means of permeation ($p>0,05$).

By analysing figure 8, one can see that all the models were permeable to insulin. During the first 15 minutes, there was a higher rate of permeation that sharply diminished after this time point and it was maintained relatively stable during the experiment time. The mean percentage of permeation of the 7-days monoculture, 7-days co-culture, 21-days monoculture, 21-days co-culture were, respectively, 12.73%; 12.14%; 12.32% and 11.87%. The highest levels of permeation achieved were, respectively, 18.32% after 4 hours; 17.34% after 4 hours; 19.56% after 4 hours; 16.45%, all after 4 hours, except for the 21-days Caco-2:Raji B model that had the highest permeation after 1 hour. This last value does not obey to the tendency of the curve and perhaps the there was some incident while collecting or quantifying the sample, since it is also the sample with higher standard deviation.

The percentage of insulin permeation of the 21-days Caco-2 monoculture was higher than the previously described by the group[106], but the permeation of the 21-days Caco-2:Raji B was in agreement with another study of the group[107]. Regarding the 7-days models, they both exhibit the same permeation profile as the 21-days models. In fact, the differences between the permeability profiles of all of the models are not significant as they all show the same tendency.

In the end of the assay, the paracellular permeability assay was performed and it revealed that the monolayer was intact – there was no detectable FITC-dextran on the basolateral compartments. This assay was performed right after the insulin assay, with only the removal of the peptide solution and the washings with PBS in between. So, this seems to point out that the cells maintained their tight junctions tight.

Since insulin has high hydrophilicity, one could expect that the protein could be partially taken up by the paracellular route. Indeed in some experiments insulin was found in the inter-cellular spaces[108], supporting this theory. However the results previously presented suggest that insulin crossed the cell barrier by some transcellular mechanism. Supporting this idea, there are some studies that claim that insulin is absorbed in the GI by endossomal compartments of enterocytes[109] while others state that the uptake of free insulin is likely to be mediated by insulin receptors[110]. Once again, looking to the hydrodynamic diameter of insulin which is approximately 56Å[111] and since the cell monolayer revealed to be intact, it seems unlikely that in this experiment the insulin passed through the pore of the tight junctions.

Comparing the effect of the presence of Raji B cells on the cultures, once more it seems to cause no detectable difference on the permeability. Since it was described that enterocytes have a mechanism of transport of insulin involving a transcellular route, it should be expected that the presence of M cells, that are known to have enhanced capacity of performing transcytosis, would cause and increase in the uptake of the drug. That was not verified leading to the suspicion that the transdifferentiation into M cells might not have happened or have not been enough to be perceived.

Considering the performance of the 7-days model on this assay, that showed the same outcomes as the traditional model, one can assume that regardless of the uptake mechanism, 7 days might be enough for the development of the cell machinery necessary to the transport of insulin. It is then reasonable to ponder this short-time model suitable for permeability studies with large-sized hydrophilic drugs. However, concerning the previous explanation for the differences in TEER between the 7 and 21-days model, one can hypothesize that the similarity between the performance of the referred model in the permeation of insulin, and even in the integrity assay with FITC-dextran, might not be verifiable using a drug with smaller size and different characteristics.

5.3. Morphological and structural characterization

The objective of the following experiments was to visually identify characteristics that define differentiated enterocytes and also M cell-like features in the co-cultures.

One of the main goals was to assess what differences could be found between the fully differentiated cells of the 21-days model and the still developing-cells of the 7-days model. Thus, some morphological traits of Caco-2 cells were analysed, namely the apical brush border and the presence of tight junctions. The microvilli of the brush border is possible to visualize through electron microscopy and the presence of tight junctions is recognisable through transmission electron microscopy and by the immunostaining of tight junction proteins such as occludin. Ocludin is a protein that mediates cell to cell adhesion, containing four transmembrane domains[99]. It has been linked to the regulation of intermembrane diffusion and paracellular diffusion of small molecules[112]. Another attribute of differentiated Caco-2 cells is the expression of enzymes such as alkaline phosphatase. In the small intestine, differentiation of the enterocytes results in increased expression and activity of several enzymes involved in digestion in which alkaline phosphatase is included. Similar increases of this brush border enzyme upon *in vitro* differentiation have also been observed in Caco-2 cells[113], so the immunostaining of alkaline phosphatase was also performed in order to assess its expression in the different culture conditions.

Regarding the features of M cells, it is described that these cells exhibit lack of microvilli at the apical surface, noticeable by electron microscopy, and may not form tight junctions as tight as Caco-2 cells do[35]. It has been described that M cells have also a decreased expression of brush border enzymes such as alkaline phosphatase[114,115], so the staining of the last two mentioned proteins was performed in the pursuit of M cells as well. Additionally, aiming to identify M cells it was also conducted the immunostainning of galectin-9. Galectin-9 is a lectin highly expressed in immune tissues that was reported to be specifically expressed on the apical surface of human M cell-like cells, representing a novel surface marker of these cells[26].

Figure 9 shows a transversal cut of a Caco-2 cell of the 7-days mono-culture model. It is possible to identify the microvilli on the apical surface of the cells and also a tight junction between the two adjacent cells. Nevertheless, the cells exhibit features of differentiated cells, which agree with the previous results, supporting the fitness of the 7-days model.

Unfortunately, the samples of the co-cultures and of the 21-days models suffered damage from the processing and it was impossible to collect clear images, so there is no term of comparison.

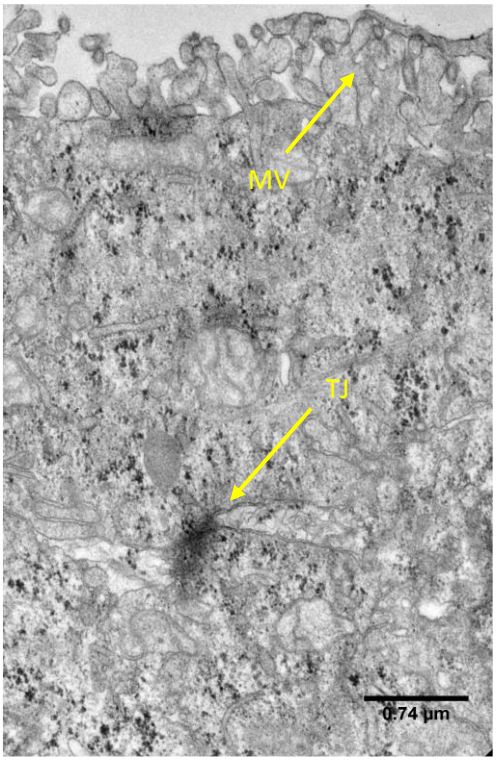

Figure 9- Transversal view of a Caco-2 cell cultured for 7 days. This image was obtained through Transmission Electron Microscopy. MV - microvilli; TJ - tight junction.

Figure 10 shows the images from the SEM analysis. Herein, it is possible to observe different phenotypes, or at least cells with different appearance, as the culture conditions vary. It is necessary to empathize that there was a drawback when culturing the 21 models, so it was possible to analyse samples with only 14 days of culture time instead of 21.

Image A is a close up on a cell monolayer of Caco-2 that were in monoculture for 7 days. Cell borders are indistinguishable, so one cannot identify the cells individually. There are a few microvilli on the cells surface and one could assume that is because of the culture period that was not enough to cells fully develop an apical brush border, when comparing with the abundant microvilli of the 14-days cultures (C and D). However, that is not the case, since the co-culture of 7 days present developed microvilli (B). So, one can assume that on (A) the microvilli are simply damaged due to the processing procedure. In fact, on image (B), besides being possible to identify developed microvilli and the individual cells, it is possible to identify a cell with less microvilli too. It is the cell signed with “M” which stands for M cell-like cell. One cannot state confidently that this cell suffered a phenotypic shift due to being in the co-culture system by presenting a single M cell feature, since it can also result from processing

procedure damage. On (C) there are visible three Caco-2 (Ca) cells and it is easy to verify cell borders since the more round shape cell has its microvilli with different orientation. These cells look morphologically fully differentiated, and when comparing these cells with the cells in (D), once can conceive that the cells pointed as "M" can be M cell-like cells due to their lack of microvilli as an outcome of the presence of Raji B lymphocytes in the culture.

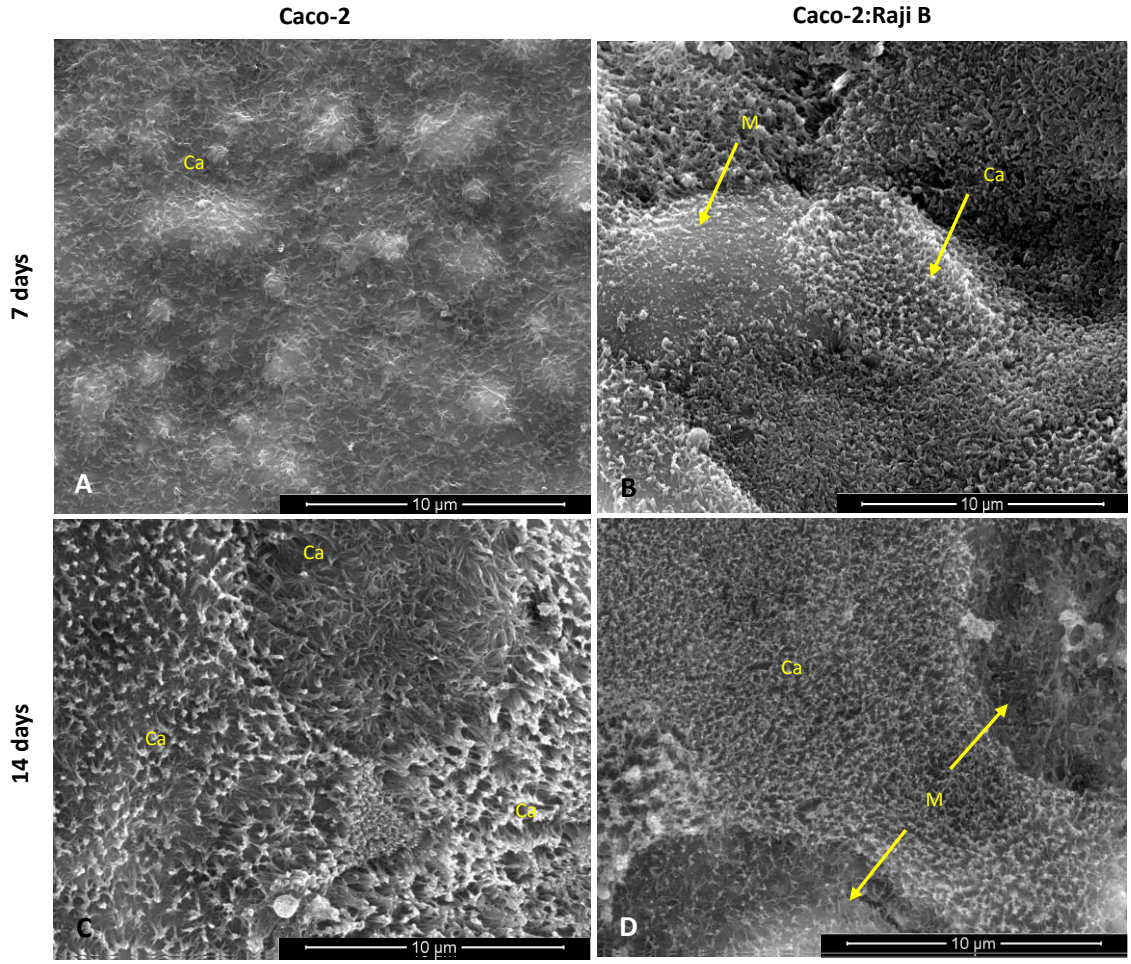

Figure 10 - Images from SEM analysis; view of cells surface in A: 7-days monoculture; B: 7-days co-culture; C: 14-days mono-culture; D: 14-days co-culture. The letters "Ca" stand for Caco-2 cell and "M" stands for M cell-like cell.

Although the accurate comparison between the 21-days and the 7-days model by SEM analysis cannot be fully described, identical studies of our research group highlighted that through SEM analyses the morphology of the 21-days cultured Caco-2 cells revealed cells with the same appearance as the cells with 14 days of culture. Nonetheless, the cells cultured for 7 days displayed microvilli (more reliably on B) and also some differences between the mono and co-culture models. Regarding the comparison between these two culture models, this was the only analysis so far that revealed some distinct features of M cell-like cells in the co-cultures.

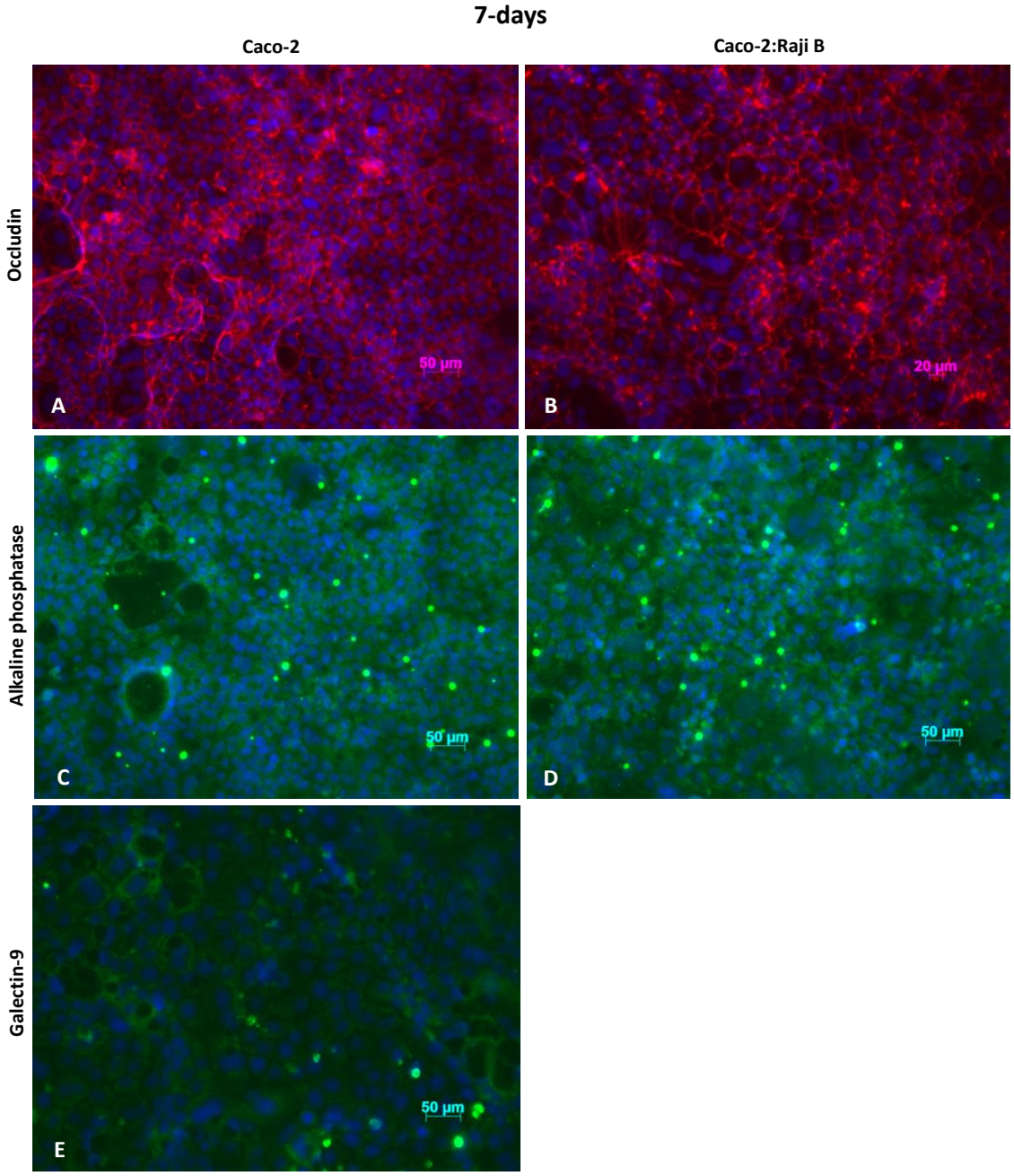

Figure 11 – Fluorescent microscopy analysis of the 7-days models. Images of the molecular staining of occludin in the monoculture model (A) and in the co-culture model (B); and the immunostainning of alkaline phosphatase of the monoculture (C) and of the co-culture (D)

Figures 11 and 12 are the result of the fluorescence microscopy studies. Images from the cultures with 7 days were firstly presented followed by the ones from de 21-days cultures.

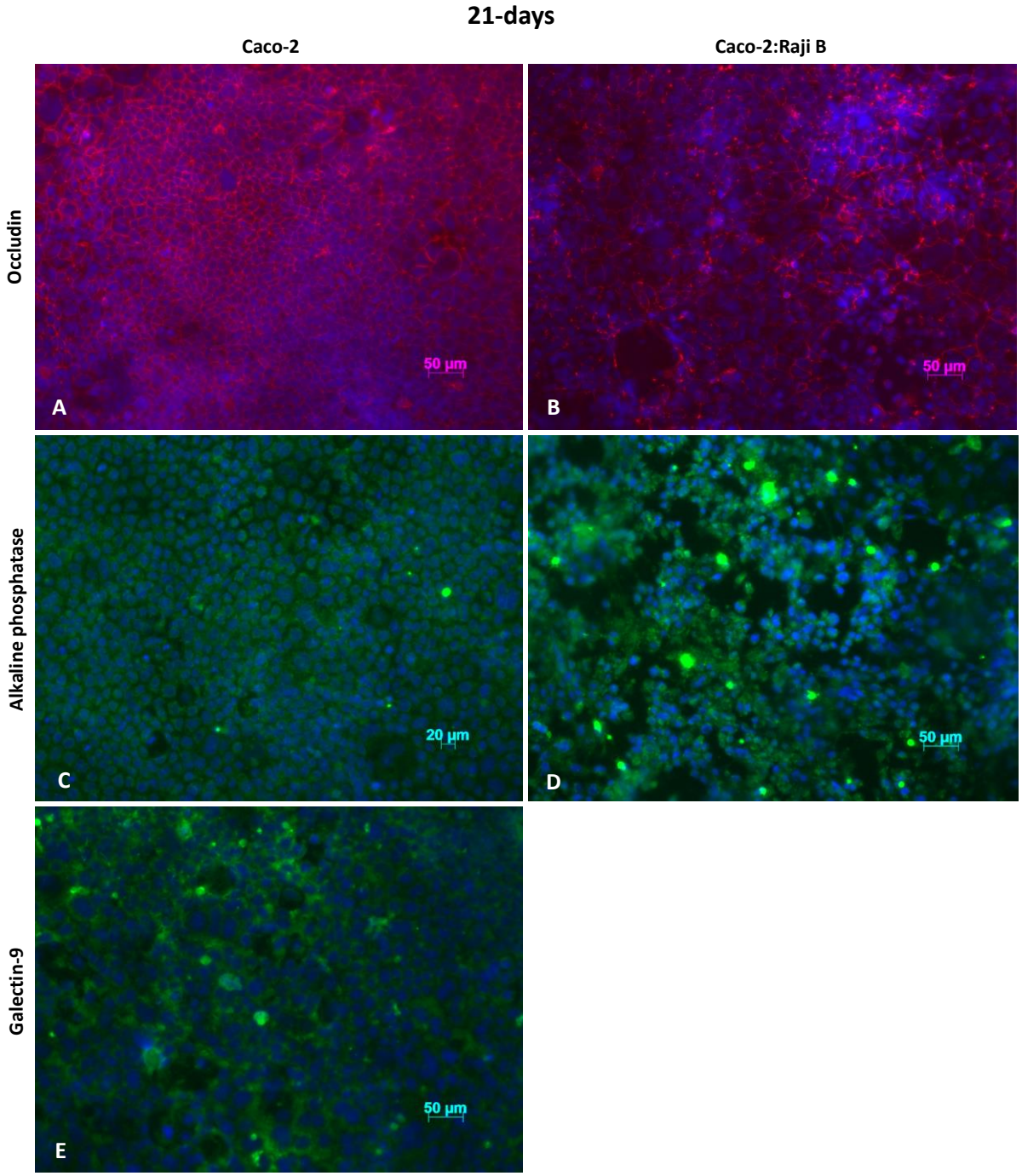

Figure 12 – Fluorescence microscopy analysis of the 21-days cultures. Images of the molecular staining of occludin in the monoculture model (A) and in the co-culture model (B); immunostainning of alkaline phosphatase of the monoculture (C) and of the co-culture (D); immunostainning of galectin-9 of the monoculture (E).

Regarding the 7 days cultures, both the occludin and alkaline phosphatase were successfully stained. So one can conclude that after 7 days the cells are differentiated enough to express

this important features. The first staining presented aimed to detect occludin, the protein of the tight junctions. The antibody successfully stained the junctions between adjacent cells in a way that is possible to distinguish individual cells and observe that they form a very compact monolayer. Even so, this is not a quantitative technique, so it is not aprecciabable if the expression of tight junctions is at the same scale as the 21 days. To visualize such difference maybe the protocol would have to be refined. The same happens with alkaline phosphatase – only determining its activity one can assess the differentiation stage. Either way, the parameters that were proposed to asses were positive, so the model of seven days expresses the same cell "key markers" as the traditional model does. More interestingly, when analysing the co-culture, the monolayers seem more intact than the ones of the 21 days model (see figure 12). If that is a consequence of damage during the staining procedure or if it is a result of a change in the cell behaviour, that did not affect the cells at this stage of development at the 7 days, is a remaining question. Concerning the staining of galectin-9, it was only possible to obtain a not so robust labeling of the monoculture (E) indicating that further optimization is required, as it will be pointed further ahead.

Regarding the 21-days cultures the first immunostaining (Figure 11 A and B) was performed to detect occludin. One can observe that they cells form a very compact monolayer especially on (A). Although the occludin staining is quite noticeable on (B), the cell monolayer integrity seems to be compromised, and that could derive from the co-culture system in which the lymphocytes could induce somehow cell detachment, or from occasionally damage caused by the staining procedure. Figure 11 (C) and (D) result from the immunostaining of the alkaline phosphatase. Indeed, Caco-2 cells express this enzyme and it seems to be localized in the cytoplasm and though one cannot see the cell membranes or junctions one can still predict that monolayer was intact (C). It is to note that these images show that alkaline phosphatase is expressed, but one cannot tell about its activity, which would be a better indicator of cell differentiation stage. In (D), where the staining of Caco-2 cells cultured with the lymphocytes is shown, it is observable once more that the integrity of the cell monolayer was compromised and the same hypothesis mentioned before can be applied to this case. Furthermore, it looks like the alkaline phosphatase staining did not occurred in the cells cytoplasm, it rather look like the cells are damaged and the enzyme was in the extracellular space. Figure 11 (E) resulted from the staining of galectin-9. Such result was really challenging to obtain since it took a lot of time to optimize de procedure. It resulted from an overnight incubation with the primary antibody and still it is not the most clear and evident staining. The fact is that the authors of the work that claimed galectin-9 as a specific M cell marker also found that this protein was solely expressed on the apical surface of M cell-like cells but could not be detected on Caco-2

cells[26]. On the other hand, it was not possible to obtain an image with the staining of galectin-9 for the co-cultures as well, so even though it was claimed that galectin-9 is a novel M-cell marker, more studies are required to demonstrate its labeling specificity and efficacy. In that sense, more experiments are being performed in order to optimize the staining procedures.

So, summarizing this section, there are no differences between the mono and co-culture models, so the fluorescence microscopy analysis did not work as an indicator for M cells; and also, there are no significant differences between the 7 and 21-days models, which confirms that the new model may be equivalent to the traditional one concerning the expression of the analysed cell markers.

Additionally, along with the referred staining procedures, the assessment of fixatives was also conducted. All the staining procedures were performed trying PFA and later methanol. Methanol was the fixating agent that led to the best results (shown in this report). The explanation may perhaps be provided by the mechanism they act by. PFA is a chemical fixative that conserves the cell structure by inducing the crosslinking of proteins, it is advisable for the staining of small proteins. On the other hand, methanol is advisable for the staining of large proteins and causes precipitation of proteins which is a physical phenomenon[116]. This last one also permeabilizes cells, while PFA requires a previous permeabilization step that in the performed experiments consisted in the use of Triton X-100. The problem of this detergent is that it is non-selective in nature and may extract proteins along with the lipids[117], so this might have been what happened. Either way, this is a process that requires a lot of optimization.

5.4. Enzymatic Activity Assessment

As it was stated before, one way to evaluate the differentiation of Caco-2 cells is to assess the activity of brush border enzymes such as alkaline phosphatase. So, to accomplished that goal the four studied cell models were subjected to this assay as described by *Ferruza et al.*, 2011[113].

Alkaline phosphatase activity assay is a simple and rapid colorimetric technique. The enzyme in alkaline environment catalyses the hydrolysis of p-Nitrophenyl phosphate (p-NPP) to inorganic phosphate and p-Nitrophenol (p-NP), a yellow soluble end-product. Then, the intensity of the coloured product is proportional to the enzyme activity and is readily measured spectrophotometrically[113].

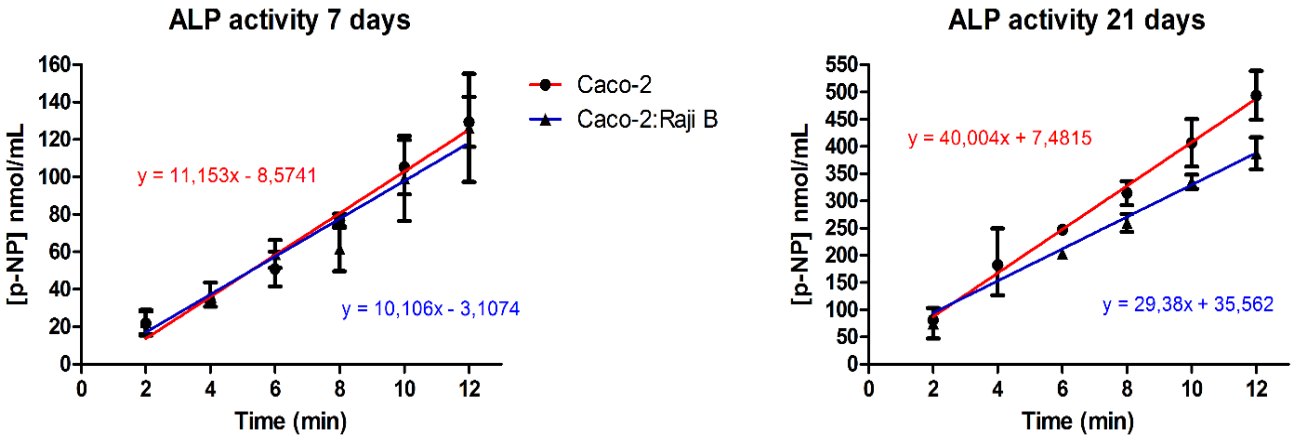

Figure 13 - Alkaline Phosphatase Activity of the four cell models. The activity is determined by angular coefficient of the linear slopes of the lines originated by the concentration of the reaction product (p-NP) plotted as a function of time.

The first step was to determine enzyme activity, which was obtained from the angular coefficient of the linear slopes of each condition plot (shown on Figure 13).

By analysing the obtained linear slopes, one can distinguish a remarkable difference between the 21 days coefficients and the 7 days coefficient, which seems to meet what was previously mentioned about the increase of the alkaline phosphatase activity along with the differentiation process. Curiously, on the 21-days models it seems to exist a difference between the monoculture a nd the co-culture, where the last one shows lower enzyme activity.

Table 1 - ALP activity

ALP ACTIVITY	7 days		21 days	
	Caco-2	Caco-2:Raji B	Caco-2	Caco-2:Raji B
mU (nmol of p-NP/mL/min)	11.153	10.106	40.04	29.38
protein (mg)	0.133 ± 0.007	0.109 ± 0.002	0.161 ± 0.031	0.122 ± 0.017
mU/mg protein	**84,061**	**93.014**	**249.207**	**240.659**

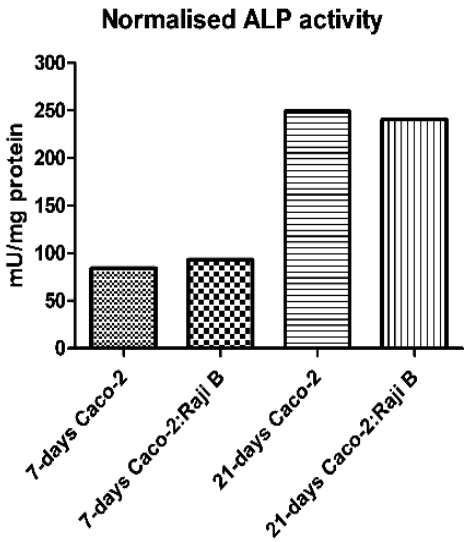

Figure 14 - Normalised ALP activity for the different culture model

After normalization to mg of protein, shown on Figure 14, it is confirmed that there was a clear decrease of enzyme activity on the 7-days models, but nothing definitive can be concluded regarding the effect of lymphocytes. Indeed it is observable a slight decrease in the ALP activity of the co-culture of 21 days that could result from the presence of a small group of M-like cells with lower ALP activity. However the experiment must be repeated, reproducibility must be obtained, so as statistical analysis, to properly evaluate de differences. Nevertheless is important to state that not only the cell models are being evaluated but also the ALP assay method itself: since the works in the literature[113-115] verified changes on the enzymatic activity on M cells of *ex vivo* samples, not in an *in vitro* model, one must assess the sensibility of such method to detect transdifferentiation. Either way, as it is noticeable on figure 10, he 7-days models showed lower enzymatic activity which indicates that, even though the immunostaining of the enzyme pointed otherwise, the cells are not differentiated enough after 7 days. This highlights the general need for quantitative studies to complement the qualitative studies, as it is the case of fluorescence microscopy images, before making any conclusions about the study subject, in this case: the differentiation stage of cells.

Furthermore, some more studies on the alkaline phosphatase activity were performed. They aimed to verify if there was differences in the enzyme activity on new different culture conditions: different ratios of Caco-2:Raji B cells and also direct contact, indirect contact between the cells and contact only with Raji B cell medium. The results are not presented on this document because they were not consistent with the previously obtained.

Regarding the 7-days model, there is one aspect that was not evaluated: the impact of the collagen type I coating. Even though the procedure was firstly being conducted, it is not presented in this work due to unexpected events that impeded the studies to be completed.

Chapter 6

Conclusions

In the present project, it was proposed to assess a 7-days Caco-2:Raji B *in vitro* model to study M cell *in vitro* transdifferentiation. In order to do so, two goals would have to be achieved, namely the validation of a 7-days cell culture model when comparing to the 21-days model, and also its capability to proportionate a phenotypic shift of Caco-2 cells into M cell-like cells.

By performing the referred experiments, several parameters were assessed leading to some conclusions, summarized in the following table.

Table 3 - Comparison of the assessed parameters between the 7-days model and the 21-days model

Parameter	7 days	21 days
Cell monolayer integrity	✓✓	✓✓✓
Permeation ability	✓✓✓	✓✓✓
Expression of differentiated cell markers	✓✓✓	✓✓✓
Enzymatic activity	✓	✓✓✓
M cell-like cells	?	?

The 7-days cell model showed similar performance in the tests when compared to the traditional model. Even though it presented lower TEER values, it displayed the same remarkable cell monolayer integrity as pointed by the paracellular permeability assays, and the same permeation ability as indicated by the insulin permeability assay. This shortened-time model also unveiled the presence of certain differentiated cell features such as: microvilli, tight junctions, and expression of alkaline phosphatase and occludin. Regarding the enzymatic activity assay, this model failed to reproduce the same results as the traditional

model, showing that cells may not be in a desirable state of differentiation required for this type of experiments. However, the non-optimal enzyme activity may not interfere with the ability of the model to mimic a physiological intestinal barrier, which is the crucial condition for the performance of drug delivery studies. However, one last parameter assessment is still not clear: the ability of the 7-days co-culture model to induce M cell differentiation. Since the expected positive control, the 21-days co-culture model showed similar ability, one cannot take definitive conclusions about the differentiation process on the 7 days culture period.

So, the outcomes of this project address mainly the 7 days monoculture model, which revealed that it might be a promising tool for the screening of new drugs by the scientific research institutions and pharmaceutical companies. Nevertheless, more studies should be performed to completely validate it. Such tests could be, for instance, permeability studies of different and more complex formulations of drugs that would not only contemplate large-sized hydrophilic compounds on their free form.

The goal of finding M cell-like cells was not clearly accomplished by all assessments of the studied parameters, so further studies are required to understand this phenomenon. Not only the detection methods must be optimized, but also, in the case of something went wrong with the establishment of the co-culture system, more conditions should be tested to overcome this problem. For instance, one can suppose that the ratio 1:2 of cell numbers of Caco-2 and Raji B is not the ideal settlement and instead a certain cell density (not number) of lymphocytes may be optimal to induce the transdifferentiation. Also, the contact time between Caco-2 cells and Raji B cells may have to be optimized. It is to note that when changing medium every three days, some of the lymphocytes were removed, and is unknown what impact the destabilization of the lymphocytes density may have on the system. Other hypothesis, is that the cells may not have been in the ideal conditions to go through this process and some factors like the passage number and origin of the cell lines could have affected the transdifferentiation. That is why more experiments are needed with the primary aim of simply detect M cell-like cells in the co-culture model and from there, a lot of interesting experiments can arise.

Besides being an improvement of the *in vitro* intestinal cell models on the resemblance with the natural intestinal tissue, such cell culture system might also be applied to the investigation of the first steps of many infectious diseases and mucosal immunity and also contribute to the screening of vaccine or drug vectors that target M cells. Moreover, it is fascinating, and of great interest, to understand how lymphocytes interact with epithelial cells: how can immune cells regulate and induce a phenotypic shift (and also functional, in the *in vivo* scenario) on the epithelium? M cells remain a mystery and their secrets must be revealed.

In the overall, the implementation of the assessed 7-days model would have huge positive impact on use of *in vitro* Caco-2 based cell models, since it would transform the current culture

model into a less laborious, less time consuming and less expensive technique, being a step forward in the quest of developing optimal intestinal cell-based engineering models.

- This page was intentionally left blank. -

References

1. Rao, J. N. & Wang, J.-Y. *Regulation of gatrointestinal mucosa growth*. (Morgan & Claypool Lifesciences, 2010).

2. Balimane, P. V & Chong, S. Cell culture-based models for intestinal permeability : a critique. *Drug Discov. Today* **10,** (2005).

3. Van der Flier, L. G. & Clevers, H. Stem cells, self-renewal, and differentiation in the intestinal epithelium. *Annu. Rev. Physiol.* **71,** 241–60 (2009).

4. Crosnier, C., Stamataki, D. & Lewis, J. Organizing cell renewal in the intestine: stem cells, signals and combinatorial control. *Nat. Rev. Genet.* **7,** 349–359 (2006).

5. Hapter, C. & Russell, M. W. in *New Bacterial Vaccines* (eds. Ellis, R. W. & Brodeur, B. R.) (Plenum, 2003).

6. Hathaway, L. J. & Kraehenbuhl, J. P. The role of M cells in mucosal immunity. *Cell. Mol. Life Sci.* **57,** 323–32 (2000).

7. Gebert, A. & Pabst, R. M cells at locations outside the gut. *Semin. Immunol.* **11,** 165–70 (1999).

8. Clark, M. a, Jepson, M. a & Hirst, B. H. Exploiting M cells for drug and vaccine delivery. *Adv. Drug Deliv. Rev.* **50,** 81–106 (2001).

9. Daugherty, A. L. & Mrsny, R. J. Transcellular uptake mechanisms of the intestinal epithelial barrier Part one. *Pharm. Sci. Technolo. Today* **2,** 144–151 (1999).

10. Swaan, P. W. Recent advances in intestinal macromolecular drug delivery via receptor-mediated transport pathways. *Pharm. Res.* **15,** (1998).

11. Apodaca, G. Endocytic traffic in polarized epithelial cells: role of the actin and microtubule cytoskeleton. *Traffic* **2,** 149–59 (2001).

12. Doherty, G. J. & McMahon, H. T. Mechanisms of endocytosis. *Annu. Rev. Biochem.* **78,** 857–902 (2009).

13. Torgersen, M. L., Skretting, G., van Deurs, B. & Sandvig, K. Internalization of cholera toxin by different endocytic mechanisms. *J. Cell Sci.* **114,** 3737–47 (2001).

14. Lu, L. & Walker, W. A. Pathologic and physiologic interactions of bacteria with the gastrointestinal epithelium. *Am. J. Clin. Nutr.* **73 ,** 1124S–1130S (2001).

15. Nicoletti, C. Unsolved mysteries of intestinal M cells. *Gut* **47,** 735–9 (2000).

16. Antunes, F., Andrade, F., Ferreira, D., Nielsen, H. M. & Sarmento, B. Models to predict intestinal absorption of therapeutic peptides and proteins. *Curr. Drug Metab.* **14,** 4–20 (2013).

17. Savidge, T. C. & Smith, M. W. in *Advances in Mucosal Immunology* (eds. Mestecky, J. *et al.*) **371,** 239–241 (Springer US, 1995).

18. Gebert, A., Rothkotter, H. & Pabst, R. M cells in Peyer's patches of the intestine. *Int. Rev. Cytol.* **I,** 91–159 (1996).

19. Torché, A.-M., Jouan, H., Le Corre, P., Albina, E., Primault, R., Jestin, A. & Le Verge, R. Ex vivo and in situ PLGA microspheres uptake by pig ileal Peyer's patch segment. *Int. J. Pharm.* **201,** 15–27 (2000).

20. Eldridge, J. H., Hammond, C. J., Meulbroek, J. A., Staas, J. K., Gilley, R. M. & Tice, T. R. Controlled vaccine release in the gut-associated lymphoid tissues. I. Orally administered biodegradable microspheres target the peyer's patches. *J. Control. Release* **11,** 205–214 (1990).

21. Jones, B. D., Ghori, N. & Falkow, S. Salmonella typhimurium initiates murine infection by penetrating and destroying the specialized epithelial M cells of the Peyer's patches. *J. Exp. Med.* **180 ,** 15–23 (1994).

22. Westphal, S., Lügering, A., von Wedel, J., von Eiff, C., Maaser, C., Spahn, T., Heusipp, G., Schmidt, M. A., … Kucharzik, T. Resistance of chemokine receptor 6-deficient mice to Yersinia enterocolitica infection: evidence of defective M-Cell formation in vivo. *Am. J. Pathol.* **172,** 671–680 (2008).

23. Ponnusamy, D., Periasamy, S., Tripathi, B. N. & Pal, A. Mycobacterium avium subsp. paratuberculosis invades through M cells and enterocytes across ileal and jejunal mucosa of lambs. *Res. Vet. Sci.* **94,** 306–312 (2013).

24. Morin, M. J., Warner, A. & Fields, B. N. A pathway for entry of reoviruses into the host through M Cells of the respiratory tract. *J. Exp. Med.* **180,** 1523–1527 (1994).

25. Rajapaksa, T. E., Bennett, K. M., Hamer, M., Lytle, C., Rodgers, V. G. J. & Lo, D. D. Intranasal M cell uptake of nanoparticles is independently influenced by targeting ligands and buffer ionic strength. *J. Biol. Chem.* **285,** 23739–46 (2010).

26. Pielage, J. F., Cichon, C., Greune, L., Hirashima, M., Kucharzik, T. & Schmidt, M. A. Reversible differentiation of Caco-2 cells reveals galectin-9 as a surface marker molecule for human follicle-associated epithelia and M cell-like cells. *Int. J. Biochem. Cell Biol.* **39,** 1886–1901 (2007).

27. Giannasca, P. J., Giannasca, K. T., Leichtner, A. M. & Neutra, M. R. Human Intestinal M Cells Display the Sialyl Lewis A Antigen Human Intestinal M Cells Display the Sialyl Lewis A Antigen. **67,** (1999).

28. Verbrugghe, P., Kujala, P., Waelput, W., Peters, P. & Cuvelier, C. Clusterin in human gut-associated lymphoid tissue, tonsils, and adenoids: localization to M cells and follicular dendritic cells. *Histochem. Cell Biol.* **129,** 311–320 (2008).

29. Sato, T., Vries, R. G., Snippert, H. J., van de Wetering, M., Barker, N., Stange, D. E., van Es, J. H., Abo, A., … Clevers, H. Single Lgr5 stem cells build crypt-villus structures in vitro without a mesenchymal niche. *Nature* **459,** 262–5 (2009).

30. De Lau, W., Kujala, P., Schneeberger, K., Middendorp, S., Li, V. S. W., Barker, N., Martens, A., Hofhuis, F., … Clevers, H. Peyer's patch M cells derived from Lgr5(+) stem cells require SpiB and are induced by RankL in cultured "miniguts". *Mol. Cell. Biol.* **32,** 3639–47 (2012).

31. Mabbott, N. a, Donaldson, D. S., Ohno, H., Williams, I. R. & Mahajan, A. Microfold (M) cells: important immunosurveillance posts in the intestinal epithelium. *Mucosal Immunol.* **6,** 666–77 (2013).

32. Gebert, A., Fassbender, S., Werner, K. & Weissferdt, A. The development of M cells in Peyer's patches is restricted to specialized dome-associated crypts. *Am. J. Pathol.* **154,** 1573–82 (1999).

33. Barker, N., van Es, J. H., Kuipers, J., Kujala, P., van den Born, M., Cozijnsen, M., Haegebarth, A., Korving, J., … Clevers, H. Identification of stem cells in small intestine and colon by marker gene Lgr5. *Nature* **449,** 1003–1007 (2007).

34. Umar, S. Intestinal stem cells. *Curr. Gastroenterol. Rep.* **12,** 340–348 (2010).

35. Araújo, F. & Sarmento, B. Towards the characterization of an in vitro triple co-culture intestine cell model for permeability studies. *Int. J. Pharm.* **458,** 128–134 (2013).

36. Lelouard, H., Sahuquet, a, Reggio, H. & Montcourrier, P. Rabbit M cells and dome enterocytes are distinct cell lineages. *J. Cell Sci.* **114,** 2077–83 (2001).

37. Smith, M. W. & Peacock, M. A. "M" cell distribution in follicle-associated epithelium of mouse peyer's patch. *Am. J. Anat.* **159,** 167–175 (1980).

38. Bhalla, D. K. & Owen, R. L. Cell renewal and migration in lymphoid follicles of Peyer's patches and cecum--an autoradiographic study in mice. *Gastroenterol. States)* **82,** (1982).

39. Knoop, K. a, Kumar, N., Butler, B. R., Sakthivel, S. K., Taylor, R. T., Nochi, T., Akiba, H., Yagita, H., … Williams, I. R. RANKL is necessary and sufficient to initiate development of antigen-sampling M cells in the intestinal epithelium. *J. Immunol.* **183,** 5738–47 (2009).

40. Galibert, L. The Involvement of Multiple Tumor Necrosis Factor Receptor (TNFR)-associated Factors in the Signaling Mechanisms of Receptor Activator of NF-kappa B, a Member of the TNFR Superfamily. *J. Biol. Chem.* **273,** 34120–34127 (1998).

41. Kanaya, T., Hase, K., Takahashi, D., Fukuda, S., Hoshino, K., Sasaki, I., Hemmi, H., Knoop, K. a, … Ohno, H. The Ets transcription factor Spi-B is essential for the differentiation of intestinal microfold cells. *Nat. Immunol.* **13,** 729–36 (2012).

42. Klemsz, M. J., McKercher, S. R., Celada, a, Van Beveren, C. & Maki, R. a. The macrophage and B cell-specific transcription factor PU.1 is related to the ets oncogene. *Cell* **61,** 113–24 (1990).

43. Sato, S., Kaneto, S., Shibata, N., Takahashi, Y., Okura, H., Yuki, Y., Kunisawa, J. & Kiyono, H. Transcription factor Spi-B-dependent and -independent pathways for the development of Peyer's patch M cells. *Mucosal Immunol.* **6,** 838–46 (2013).

44. Savidge, T. C. The life and times of an intestinal M cell. *Trends Microbiol.* **4,** 301–306 (1996).

45. Kerneis, S. Conversion by Peyer's Patch Lymphocytes of Human Enterocytes into M Cells that Transport Bacteria. *Science.* **277,** 949–952 (1997).

46. Sharma, R., Schumacher, U. & Adam, E. Lectin histochemistry reveals the appearance of M-cells in Peyer's patches of SCID mice after ayngeneic normal bone marrow transplantation. *J. Histochem. Cytochem.* **46,** 143–148 (1998).

47. Golovkina, T. V. Organogenic Role of B Lymphocytes in Mucosal Immunity. *Science.* **286,** 1965–1968 (1999).

48. Cook, D. N., Prosser, D. M., Forster, R., Zhang, J., Kuklin, N. a, Abbondanzo, S. J., Niu, X. D., Chen, S. C., … Lira, S. a. CCR6 mediates dendritic cell localization, lymphocyte homeostasis, and immune responses in mucosal tissue. *Immunity* **12,** 495–503 (2000).

49. Iwasaki, A. & Kelsall, B. L. Localization of Distinct Peyer's Patch Dendritic Cell Subsets and Their Recruitment by Chemokines Macrophage Inflammatory Protein (Mip)-3α, Mip-3β, and Secondary Lymphoid Organ Chemokine. *J. Exp. Med.* **191 ,** 1381–1394 (2000).

50. Ebisawa, M., Hase, K., Takahashi, D., Kitamura, H., Knoop, K. a, Williams, I. R. & Ohno, H. CCR6hiCD11c(int) B cells promote M-cell differentiation in Peyer's patch. *Int. Immunol.* **23,** 261–9 (2011).

51. Kobayashi, A., Donaldson, D. S., Erridge, C., Kanaya, T., Williams, I. R., Ohno, H., Mahajan, A. & Mabbott, N. A. The functional maturation of M cells is dramatically reduced in the Peyer's patches of aged mice. *Mucosal Immunol.* **6,** 1027–37 (2013).

52. Tumanov, a. V., Kuprash, D. V., Mach, J. a., Nedospasov, S. a. & Chervonsky, a. V. Lymphotoxin and TNF Produced by B Cells Are Dispensable for Maintenance of the Follicle-Associated Epithelium but Are Required for Development of Lymphoid Follicles in the Peyer's Patches. *J. Immunol.* **173,** 86–91 (2004).

53. Wang, J., Lopez-Fraga, M., Rynko, A. & Lo, D. D. {TNFR} and LTβR agonists induce follicle-associated epithelium and M cell specific genes in rat and human intestinal epithelial cells. *Cytokine* **47,** 69–76 (2009).

54. Rumbo, M., Sierro, F., Debard, N., Kraehenbuhl, J.-P. & Finke, D. Lymphotoxin β receptor signaling induces the chemokine {CCL20} in intestinal epithelium. *Gastroenterology* **127,** 213–223 (2004).

55. Hsieh, E. H., Fernandez, X., Wang, J., Hamer, M., Calvillo, S., Croft, M., Kwon, B. S. & Lo, D. D. CD137 is required for M cell functional maturation but not lineage commitment. *Am. J. Pathol.* **177,** 666–76 (2010).

56. Wang, J., Gusti, V., Saraswati, A. & Lo, D. D. Convergent and divergent development among M cell lineages in mouse mucosal epithelium. *J. Immunol.* **187,** 5277–85 (2011).

57. Debard, N., Sierro, F., Browning, J. & Kraehenbuhl, J. P. Effect of mature lymphocytes and lymphotoxin on the development of the follicle-associated epithelium and M cells in mouse Peyer's patches. *Gastroenterology* **120,** 1173–82 (2001).

58. Sierro, F., Dubois, B., Coste, A., Kaiserlian, D., Kraehenbuhl, J.-P. & Sirard, J.-C. Flagellin stimulation of intestinal epithelial cells triggers CCL20-mediated migration of dendritic cells. *Proc. Natl. Acad. Sci.* **98 ,** 13722–13727 (2001).

59. Meynell, H. M., Thomas, N. W., James, P. S., Holland, J., Taussig, M. J., Nicoletti, C. & Up-regulation, C. Up-regulation of microsphere transport across the follicle-associated epithelium of Peyer ' s patch by exposure to Streptococcus pneumoniae R36a. 611–619

60. Gebert, A., Hach, G. & Bartels, H. Co-localization of vimentin and cytokeratins in M-cells of rabbit gut-associated lymphoid tissue (GALT). *Cell Tissue Res.* **269,** 331–340 (1992).

61. Gebert, a. Identification of M-cells in the rabbit tonsil by vimentin immunohistochemistry and in vivo protein transport. *Histochem. Cell Biol.* **104,** 211–20 (1995).

62. Tahoun, A., Mahajan, S., Paxton, E., Malterer, G., Donaldson, D. S., Wang, D., Tan, A., Gillespie, T. L., … Mahajan, A. Salmonella transforms follicle-associated epithelial cells into M cells to promote intestinal invasion. *Cell Host Microbe* **12,** 645–56 (2012).

63. Hernandez, L. D., Hueffer, K., Wenk, M. R. & Galán, J. E. Salmonella modulates vesicular traffic by altering phosphoinositide metabolism. *Science* **304,** 1805–7 (2004).

64. Patel, J. C., Hueffer, K., Lam, T. T. & Galán, J. E. Diversification of a Salmonella Virulence Protein Function by Ubiquitin-Dependent Differential Localization. *Cell* **137,** 283–294 (2009).

65. Knodler, L. a, Finlay, B. B. & Steele-Mortimer, O. The Salmonella effector protein SopB protects epithelial cells from apoptosis by sustained activation of Akt. *J. Biol. Chem.* **280,** 9058–64 (2005).

66. Man, A. L., Lodi, F., Bertelli, E., Regoli, M., Pin, C., Mulholland, F., Satoskar, A. R., Taussig, M. J. & Nicoletti, C. Macrophage migration inhibitory factor plays a role in the regulation of microfold (M) cell-mediated transport in the gut. *J. Immunol.* **181,** 5673–80 (2008).

67. Perry, M. & Whyte, A. Immunology of the tonsils. *Immunol. Today* **19,** 414–421 (1998).

68. Fujimura, Y. Evidence of M cells as portals of entry for antigens in the nasopharyngeal lymphoid tissue of humans. *Virchows Arch.* **436,** 560–6 (2000).

69. Kiyono, H. & Fukuyama, S. NALT- versus Peyer's-patch-mediated mucosal immunity. *Nat. Rev. Immunol.* **4,** 699–710 (2004).

70. Debertin, A. S., Tschering, T., Tonjes, H., Kleeman, W. J., Troger, H. D. & Pabst, R. Nasal-associated lymphoid tissue (NALT): frequency and localization in young children. *Clin. Exp. Immunol.* **134,** 503–507 (2003).

71. Gebert, A. M-cells in the rabbit tonsil exhibit distinctive glycoconjugates in their apical membranes. *J. Histochem. Cytochem.* **44 ,** 1033–1042 (1996).

72. Kim, D.-Y., Sato, A., Fukuyama, S., Sagara, H., Nagatake, T., Kong, I. G., Goda, K., Nochi, T., … Kiyono, H. The airway antigen sampling system: respiratory M cells as an alternative gateway for inhaled antigens. *J. Immunol.* **186,** 4253–62 (2011).

73. Rock, J. R., Onaitis, M. W., Rawlins, E. L., Lu, Y., Clark, C. P., Xue, Y., Randell, S. H. & Hogan, B. L. M. Basal cells as stem cells of the mouse trachea and human airway epithelium. *Proc. Natl. Acad. Sci.* (2009). at <http://www.pnas.org/content/early/2009/07/21/0906850106.abstract>

74. Klein, T.-O., Soll, B. a, Issel, B. F. & Fraser, C. Bronchus-associated lymphoid tissue lymphoma and Mycobacterium tuberculosis infection: an unusual case and a review of the literature. *Respir. Care* **52,** 755–8 (2007).

75. Pabst, R. & Tschernig, T. Bronchus-associated lymphoid tissue: an entry site for antigens for successful mucosal vaccinations? *Am. J. Respir. Cell Mol. Biol.* **43,** 137–41 (2010).

76. Toyoshima, M., Chida, K. & Sato, A. Antigen uptake and subsequent cell kinetics in bronchus-associated lymphoid tissue. *Respirology* **5,** 141–145 (2000).

77. Teitelbaum, R., Schubert, W., Gunther, L., Kress, Y., Macaluso, F., Pollard, J. W., McMurray, D. N. & Bloom, B. R. The M Cell as a Portal of Entry to the Lung for the Bacterial Pathogen Mycobacterium tuberculosis. *Immunity* **10,** 641–650 (1999).

78. Cencič, A. & Langerholc, T. Functional cell models of the gut and their applications in food microbiology — A review. *Int. J. Food Microbiol.* **141, Suppl,** S4–S14 (2010).

79. Polli, J. E. in vitro studies are sometimes better than conventional human pharmacokinetic in vivo studies in assessing bioequivalence of immediate-release solid oral dosage forms. *AAPS J.* **10,** 289–299 (2008).

80. Balimane, P. V, Chong, S. & Morrison, R. A. Current methodologies used for evaluation of intestinal permeability and absorption. *J. Pharmacol. Toxicol. Methods* **44,** 301–312 (2000).

81. Smetanová, L., Stětinová, V., Svoboda, Z. & Kvetina, J. Caco-2 cells, biopharmaceutics classification system (BCS) and biowaiver. *Acta Medica (Hradec Kralove)* **54,** 3–8 (2011).

82. Ungell, A.-L. B. Caco-2 replace or refine? *Drug Discov. Today Technol.* **1,** 423–430 (2004).

83. Yamashita, S., Furubayashi, T., Kataoka, M., Sakane, T., Sezaki, H. & Tokuda, H. Optimized conditions for prediction of intestinal drug permeability using Caco-2 cells. *Eur. J. Pharm. Sci.* **10,** 195–204 (2000).

84. Sarmento, B., Andrade, F., Silva, S. B. da, Rodrigues, F., das Neves, J. & Ferreira, D. Cell-based in vitro models for predicting drug permeability. *Expert Opin. Drug Metab. Toxicol.* **8,** 607–621 (2012).

85. Sun, H., Chow, E. C. Y., Liu, S., Du, Y. & Pang, K. S. The Caco-2 cell monolayer: usefulness and limitations. *Expert Opin. Drug Metab. Toxicol.* **4,** 395–411 (2008).

86. Li, N., Wang, D., Sui, Z., Qi, X., Ji, L., Wang, X. & Yang, L. Development of an improved three-dimensional in vitro intestinal mucosa model for drug absorption evaluation. *Tissue Eng. Part C* **19,** 708–719 (2013).

87. Cai, Y., Xu, C., Chen, P., Hu, J., Hu, R., Huang, M. & Bi, H. Development, validation, and application of a novel 7-day Caco-2 cell culture system. *J. Pharmacol. Toxicol. Methods* 1–7 (2014). doi:10.1016/j.vascn.2014.07.001

88. Lentz, K. a, Hayashi, J., Lucisano, L. J. & Polli, J. E. Development of a more rapid, reduced serum culture system for Caco-2 monolayers and application to the biopharmaceutics classification system. *Int. J. Pharm.* **200,** 41–51 (2000).

89. Chong, S., Dando, S. & Morrison, R. Evaluation of Biocoat® Intestinal Epithelium Differentiation Environment (3-Day Cultured Caco-2 Cells) as an Absorption Screening Model with Improved Productivity. *Pharm. Res.* **14,** 1835–1837 (1997).

90. Sevin, E., Dehouck, L., Fabulas-da Costa, a, Cecchelli, R., Dehouck, M. P., Lundquist, S. & Culot, M. Accelerated Caco-2 cell permeability model for drug discovery. *J. Pharmacol. Toxicol. Methods* **68,** 334–9 (2013).

91. Swiderek, M. S., Mannuzza, F. J. & Park, T. O. Effects of ECM Proteins on Barrier Formation in Caco-2 Cells.

92. Peng, Y., Yadava, P., Heikkinen, A. T., Parrott, N. & Railkar, A. Applications of a 7-day Caco-2 cell model in drug discovery and development. *Eur. J. Pharm. Sci.* **56,** 120–30 (2014).

93. Gullberg, E., Leonard, M., Karlsson, J., Hopkins, A. M., Brayden, D., Baird, A. W. & Artursson, P. Expression of specific markers and particle transport in a new human intestinal M-cell model. *Biochem. Biophys. Res. Commun.* **279,** 808–813 (2000).

94. Des Rieux, A., Fievez, V., Momtaz, M., Detrembleur, C., Alonso-Sande, M., Van Gelder, J., Cauvin, A., Schneider, Y.-J. & Préat, V. Helodermin-loaded nanoparticles: characterization and transport across an in vitro model of the follicle-associated epithelium. *J. Control. Release* **118,** 294–302 (2007).

95. Shah, P., Jogani, V., Bagchi, T. & Misra, A. Role of Caco-2 cell monolayers in prediction of intestinal drug absorption. *Biotechnol. Prog.* **22,** 186–98 (2006).

96. Sarmento, B., Ribeiro, A., Veiga, F. & Ferreira, D. Development and validation of a rapid reversed-phase HPLC method for the determination of insulin from nanoparticulate systems. *Biomed. Chromatogr.* **20,** 898–903 (2006).

97. Lowry, O. H., Rosebrough, N. J., Farr, A. L. & Randall, R. J. Protein measurement with the folin phenol reagent. *J. Biol. Chem.* **193,** 265–275 (1951).

98. D'Souza, V. M., Shertzer, H. G., Menon, A. G. & Pauletti, G. M. High glucose concentration in isotonic media alters caco-2 cell permeability. *AAPS PharmSci* **5,** E24 (2003).

99. Ulluwishewa, D., Anderson, R. C., McNabb, W. C., Moughan, P. J., Wells, J. M. & Roy, N. C. Regulation of tight junction permeability by intestinal bacteria and dietary components. *J. Nutr.* **5,** 769–776 (2011).

100. Silva, C. M., Veiga, F., Ribeiro, A. J., Zerrouk, N. & Arnaud, P. Effect of chitosan-coated alginate microspheres on the permeability of Caco-2 cell monolayers. *Drug Dev. Ind. Pharm.* **32,** 769–776 (2006).

101. Watson M. Warhurst, G., C. J. R. Functional modeling of tight junctions in intestinal cell monolayers using polyethylene glycol oligomers. *Am. J. Physiol. - Cell Physiol.* **281,** C388–C397 (2001).

102. Sigma-Aldrich. *Fluorescein isothiocyanate-dextran: product information*. (1997).

103. Hilgers, A., Conradi, R. & Burton, P. Caco-2 cell monolayers as a model for drug transport across the intestinal mucosa. *Pharm. Res.* **7,** 902–910 (1990).

104. Chiba, H., Osanai, M., Murata, M., Kojima, T. & Sawada, N. Transmembrane proteins of tight junctions. *Biochim. Biophys. Acta - Biomembr.* **1778,** 588–600 (2008).

105. Des Rieux, A., Ragnarsson, E. G. E., Gullberg, E., Préat, V., Schneider, Y.-J. & Artursson, P. Transport of nanoparticles across an in vitro model of the human intestinal follicle associated epithelium. *Eur. J. Pharm. Sci.* **25,** 455–65 (2005).

106. Fonte, P., Nogueira, T., Gehm, C., Ferreira, D. & Sarmento, B. Chitosan-coated solid lipid nanoparticles enhance the oral absorption of insulin. *Drug Deliv. Transl. Res.* **1,** 299–308 (2011).

107. Antunes, F., Andrade, F., Araújo, F., Ferreira, D. & Sarmento, B. Establishment of a triple co-culture in vitro cell models to study intestinal absorption of peptide drugs. *Eur. J. Pharm. Biopharm.* **83,** 427–35 (2013).

108. Tang, C., Yu, J., Yin, L., Yin, C. & Pei, Y. Transport of insulin in modified valia-chien chambers and Caco-2 cell monolayers. *Drug Dev. Ind. Pharm.* **33,** 449–456 (2007).

109. Ziv, E. & Bendayan, M. Intestinal absorption of peptides through the enterocytes. *Microsc. Res. Tech.* **49,** 346–352 (2000).

110. Thompson, C., Cheng, W., Gadad, P., Skene, K., Smith, M., Smith, G., McKinnon, A. & Knott, R. Uptake and transport of novel amphiphilic polyelectrolyte-insulin nanocomplexes by Caco-2 cells—towards oral insulin. *Pharm. Res.* **28,** 886–896 (2011).

111. Chien, Y. W. Human insulin: basic sciences to therapeutic uses. *Drug Dev. Ind. Pharm.* **22,** 753–789 (1996).

112. Balda, M. S., Whitney, J. A., Flores, C., González, S., Cereijido, M. & Matter, K. Functional dissociation of paracellular permeability and transepithelial electrical resistance and disruption of the apical-basolateral intramembrane diffusion barrier by expression of a mutant tight junction membrane protein. *J. Cell Biol.* **134 ,** 1031–1049 (1996).

113. Ferruzza, S., Rossi, C., Scarino, M. L. & Sambuy, Y. A protocol for in situ enzyme assays to assess the differentiation of human intestinal Caco-2 cells. *Toxicol. In Vitro* **26,** 1247–51 (2012).

114. Owen, R. L. & Bhalla, D. K. Cytochemical analysis of alkaline phosphatase and esterase activities and of lectin-binding and anionic sites in rat and mouse Peyer's patch M cells. *Am. J. Anat.* **168,** 199–212 (1983).

115. Brown, D., Cremaschi, D., James, P. S., Rossetti, C. & Smith, M. W. Brush-border membrane alkaline phosphatase activity in mouse Peyer's patche follicle-associated enterocytes. *J. Physiol.* 81–88 (1990).

116. Snider, J. Thermo Scientific - Fixation strategies. (2014). at <http://www.piercenet.com/method/fixation-strategies-formulations>

117. Jamur, M. C. & Oliver, C. in *Immunocytochemical Methods and Protocols* (eds. Oliver, C. & Jamur, M. C.) **588,** 63–66 (Humana Press, 2010).

118. Hubatsch, I., Ragnarsson, E. G. E. & Artursson, P. Determination of drug permeability and prediction of drug absorption in Caco-2 monolayers. *Nat. Protoc.* **2,** 2111–9 (2007).